Effects of Aging on the Molecular Profile of Cultured Tendon Cells

Carrie E. Barnum, Julianne Huegel, Louis J. Soslowsky, Andrew F. Kuntz
McKay Orthopaedic Research Laboratory, University of Pennsylvania, Philadelphia, PA

DISCLOSURES: Barnum C (N), Huegel J (N), Soslowsky LJ (N), Kuntz AF (N)

INTRODUCTION: Rotator cuff tears affect millions of individuals each year, with a higher incidence in the elderly. Although surgical repair can improve function and reduce pain, rotator cuff repair failure is common [1]. To improve surgical outcomes, biologic augmentation via delivery of cells or growth factors has been investigated [2-4]. Recently, autologous biceps cells delivered via nanofibrous scaffold to the repair site during supraspinatus repair were shown to improve healing in juvenile and aged rats, but did not affect healing in adult rats [5]. However, the molecular mechanisms behind these differential effects are not well understood. Therefore, the objective of this study was to determine the differences in the RNA signature of primary tendon-derived cells cultured from the long head of the biceps of juvenile, adult, and aged animals. Our hypotheses were: 1) tendon-derived cells from juvenile animals would exhibit a molecular profile more characteristic of stem cells than tendon-derived cells from adult or aged animals, and 2) tendon-derived cells from aged rats would have increased expression of genes associated with tendon homeostasis and differentiation compared to cells derived from juvenile or adult rats.

METHODS: 27 Fisher (F344) rats were used (IACUC approved) across three age groups: juvenile (4 weeks), adult (8 months), and aged (16 months) (n=9/age group). Animals were sacrificed and the intra-articular biceps tendons were collected. *Cell Culture*: Biceps tendon cells were harvested from the tissue via morselization and cell migration. Cells were expanded in culture using basal media and split at confluence. Subcultured (P1) cells were allowed to reach 75-85% confluence (average 12 days in culture) at which time they were lysed and homogenized in TRIzol. *RNA Isolation*: RNA was isolated using the TRIspin method and processed via RNA Clean & Concentrator 5 columns (Zymo Research). *Rat Transcriptome Array and Bioinformatics Analysis*: cDNA made with 250ng of RNA using the Affymetrix WT PLUS Kit and was run on a Clariom™ D Rat Transcriptome Array 1.0 (Applied Biosystems, n=5/age group). Bioinformatics processing was performed using Transcriptome Analysis Console Software and DAVID analysis (cut-offs set at |FC|>2 and $p<0.05$ for all pair-wise age comparisons). *qRT-PCR*: Reverse transcription was performed using a High Capacity cDNA Reverse Transcription Kit (Applied Biosystems). To validate microarray results, qPCR was run in quadruplicate using TaqMan Assays on a QuantStudio 12K Flex Real-Time PCR system (ThermoFisher, n=8/age group). Data was analyzed using the ΔΔCt method, and expression levels were compared between age groups with one-way ANOVAs and post-hoc Tukey tests. *Cell Staining*: At 50% confluence, P1 cells were fixed, permeabilized, and stained with Alexa Fluor 488 Phalloidin and DAPI. Slides were imaged with a Leica TCS SP8 Multiphoton Confocal.

RESULTS: Principle component analysis demonstrated that cell expression profiles grouped into distinct regions by age (Fig. 1). The majority of gene expression clustered into six distinct patterns when comparing between ages (data not shown). The majority of differential gene expression exists between juvenile and aged cells (640 genes significantly decreased, 531 increased), while the fewest differences exist between adult and aged cells (54 genes significantly decreased, 101 genes increased). Comparison of juvenile cells to adult cells identified 216 significantly increased genes and 203 significantly decreased genes. No qualitative differences were observed in cell morphology between age groups (data not shown). Gene ontology identified differences in genes related to: 1) cell adhesion, wound healing, and chondrocyte differentiation between juvenile and adult cells, 2) cell division and cell adhesion between juvenile and aged cells, and 3) wound healing and vasculogenesis between adult and aged cells. qPCR confirmed that genes associated with stemness are downregulated with age, including *Postn*, *Fgf10*, *Osr1*, and *Gpmnb* (Fig. 2). Additionally, genes related to inflammation are differentially expressed with age, including increased *Cd28* and *Cd200* expression and decreased *Il6* and *Il6st* expression (Fig. 3).

DISCUSSION: Results demonstrate distinct molecular profiles for juvenile, adult, and aged biceps tendon-derived cells. Juvenile cells showed increased expression of genes associated with mesenchymal stem cells, such as *Postn and Fgf10*, supporting our first hypothesis. Furthermore, although stem cell associated markers are present in both juvenile and adult cells, they are significantly decreased in aged cells, suggesting that a greater population of aged tendon cells may have terminally differentiated. However, contrary to our second hypothesis, there were no consistent increases in the expression of tendon markers in aged cells, suggesting that there may be significant population heterogeneity. Interestingly, aged cells demonstrate a decreased pro-inflammatory signature, including decreased expression of pro-inflammatory cytokine *Il6* and its signaling receptor *Il6st*, as well as an increased anti-inflammatory milieu, including increases in both *Cd28* and *Cd200* expression compared to juvenile cells. Previous work demonstrated that Il6-null mice (simulating an aged phenotype) have increased native tendon mechanical properties [6], but show a similar healing response as WT mice [7], suggesting a role for this cytokine in how delivered cells integrate into and contribute to new tendon formation. This study specifically explored RNA level changes in biceps tendons in culture, and we have not yet shown that these findings relate to changes at the protein level. However, these age-specific expression signatures can begin to uncover the mechanisms behind functional differences previously shown between age groups after cell delivery [5]. Future research will investigate protein level changes as well as how these changes relate to functional differences in tendon healing with age. It will be important to discern how both population heterogeneity and inflammation affect the contribution of scaffold-delivered biceps cells for rotator cuff repair.

SIGNIFICANCE/CLINICAL RELEVANCE: We previously demonstrated age-specific differences in supraspinatus healing after autologous biceps cell delivery [5]; the current study demonstrates that these cell populations display distinct molecular differences. These differences should be considered when addressing musculoskeletal regenerative medicine, particularly in the context of augmented tendon repair. Furthermore, modulating the molecular profile of adult or aged cells may further improve tendon repair.

REFERENCES: [1] Galatz LM et al. J Bone Joint Surg Am, 2004. [2] Hernigou P et al. Int Orthop, 2014. [3] Chen JM et al. Tissue Eng, 2007. [4] Longo UG et al. Br Med Bull, 2010. [5] Huegel J et al. J Orthop Res. 2017. [6] Lin TW et al. J Biomech. 2005. [7] Lin TW et al. J Biomech. 2006.

ACKNOWLEDGEMENTS: This study was supported by the American Shoulder and Elbow Surgeons Research Grant. We would like to thank Dr. Snehal Shetye for his help with the cluster analysis.

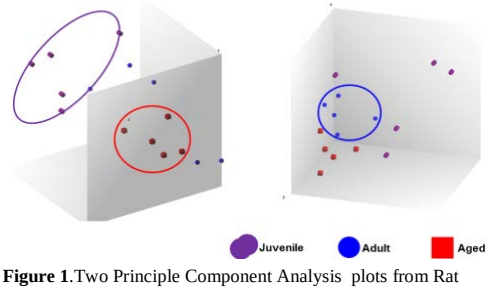

Figure 1.Two Principle Component Analysis plots from Rat Transcriptome Analysis. Juvenile cells shown as purple cylinders, adult cells are shown as blue spheres, and aged cells are represented as red cubes. Age groups are circled to demonstrate distinct clusters.

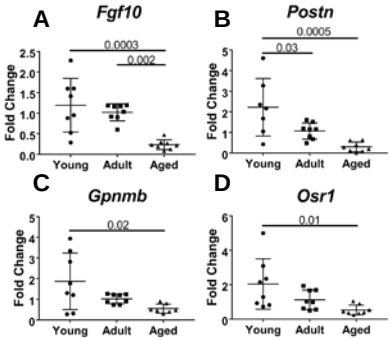

Figure 2. Decreased expression of stem related mRNAs measured via qPCR. (A) *Fgf10* (B) *Postn* (C) *Gpnmb* and (D) *Osr1* expression decreased with aging. Significance is denoted with solid lines (n=8/group).

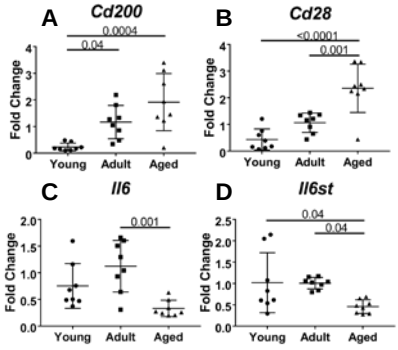

Figure 3. qPCR confirms changes in inflammatory response with age. (A) *Cd200* and (B) *Cd28* increased with age, while (C) *Il6* decreased in aged cells only and (D) *Il6st* decreased with aging. Significance is denoted with solid lines (n=8/group).

Differential Roles for Decorin and Biglycan in Tendon Aging

Beach ZM[1], Dekhne M[1], Rodriguez AR[1], Weiss SN[1], Shetye SS[1], Adams TH[2], Adams SM[2], Sun M[2], Birk DE[2], Soslowsky LJ[1]
[1]McKay Orthopaedic Laboratory, University of Pennsylvania, Philadelphia, PA
[2]Department of Molecular Pharmacology and Physiology, University of South Florida, Tampa, FL

Disclosures: Zakary M. Beach (N), Mihir Dekhne (N), Ashley R. Rodriguez (N), Stephanie N. Weiss (N), Snehal S. Shetye (N), Thomas H. Adams (N), Sheila M. Adams (N), Mei Sun (N), David E. Birk (N), Louis J. Soslowsky (N)

INTRODUCTION: Tendon injuries occur more commonly with increasing age [1], yet the mechanisms underlying the process of tendon aging are unclear. Decorin (Dcn) and biglycan (Bgn) are two small leucine-rich proteoglycans (SLRPs) that are regulators of collagen fibrillogenesis and are highly expressed during tendon development [2]. The absence of Dcn has been shown to prevent the normal decline in mechanics with decreasing age [3], while the inducible deletion of Bgn [4] and compound Dcn/Bgn [5] resulted in reduced mechanical and structural properties in mature tendon. However, the roles of Dcn and Bgn on tendon aging, independent of their influence on development, are unknown. Therefore, the objective of this study was to determine the differential roles of Dcn and Bgn during tendon aging. Due to the detrimental effects of Dcn on tendon aging, we hypothesized that the Dcn- and Dcn/Bgn-null mice will show a reduced impact of aging on mechanical and structural properties compared to WT and Bgn-null mice.

METHODS: Female $Dcn^{+/+}/Bgn^{+/+}$ control (WT, n=32), $Dcn^{flox/flox}$ (I-$Dcn^{-/-}$, n=32), $Bgn^{flox/flox}$ (I-$Bgn^{-/-}$, n=32), and compound $Dcn^{flow/flox}/Bgn^{flox/flox}$ (I-$Dcn^{-/-}/Bgn^{-/-}$, n=32), mice with a tamoxifen (TM) inducible Cre, (B6.129-Gt(ROSA)26Sortm1(cre/ERT2)Tyj/J, Jackson Labs) were utilized [5] (IACUC approved). Cre excision of the conditional alleles was induced in mature (120 day) [5] mice via three consecutive daily IP injections of tamoxifen (4.5mg/40g body weight). WT mice received TM injections to control for potential side effects. Mice were euthanized at 300 and 570 days of age (n=16/group/age). The patellar tendon-bone complex from one limb of each animal was dissected and prepared for mechanical testing [6]. Tendons (n=16) were subjected to a viscoelastic testing protocol of three stress relaxations, each followed by frequency sweeps, with the test culminating in a ramp-to-failure. Percent relaxation was quantified for each stress-relaxation. Samples for transmission electron microscopy (TEM) analysis of fibril structure (n=4) were fixed *in situ* [5]. Cross sections through the midsubstance of the patellar tendon were examined at 80 kV. Fibril diameter was measured using images from the center of the tendon. Histological sections of the patellar tendon-bone complex (n=4) were prepared using standard techniques. Cell shape and cellularity were calculated using commercial software (Bioquant). A two-way ANOVA was performed followed by Bonferroni post-hoc analysis to evaluate the effect of genotype and age on tendon mechanics. Kolmogorov-Smirnov tests were used for the analysis of TEM and histology data. Significance was set at $p<0.05$.

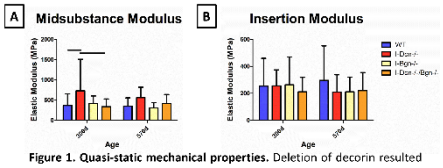

Figure 1. Quasi-static mechanical properties. Deletion of decorin resulted in increased midsubstance elastic modulus at 300d compared to WT and I-$Dcn^{-/-}/Bgn^{-/-}$ (A). No differences were found at 570d or in the insertion (B).

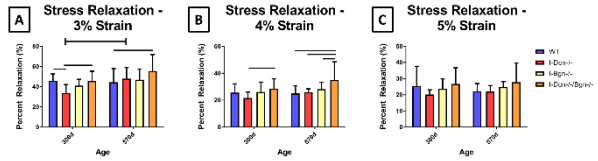

Figure 2. Stress Relaxation. I-$Dcn^{-/-}/Bgn^{-/-}$ showed increased stress relaxation at 3% and 4% strain at 300d & 570d (A, B). At 3% strain, 570d I-$Dcn^{-/-}$ stress relaxation was increased vs 300d I-$Dcn^{-/-}$ (A). No changes were seen at 5% strain (C).

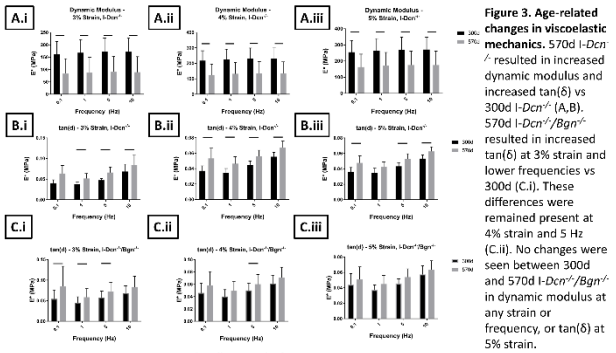

Figure 3. Age-related changes in viscoelastic mechanics. 570d I-$Dcn^{-/-}$ resulted in increased dynamic modulus and increased tan(δ) vs 300d I-$Dcn^{-/-}$ (A,B). 570d I-$Dcn^{-/-}/Bgn^{-/-}$ resulted in increased tan(δ) at 3% strain and lower frequencies vs 300d (C.i). These differences were remained present at 4% strain and 5 Hz (C.ii). No changes were seen between 300d and 570d I-$Dcn^{-/-}/Bgn^{-/-}$ in dynamic modulus at any strain or frequency, or tan(δ) at 5% strain.

RESULTS: Genotype significantly affected midsubstance modulus, while age and the interaction between age and genotype did not. Induced deletion of *Dcn* resulted in increased midsubstance elastic modulus at 300d (Fig. 1A) versus WT and I-$Dcn^{-/-}/Bgn^{-/-}$. These differences were not present at 570d or in the insertion region (Fig. 1B). Stress relaxation at 3% strain (Fig. 2A) revealed genotype, age, and the interaction between genotype and age as significant. I-$Dcn^{-/-}/Bgn^{-/-}$ showed increased percent relaxation versus WT, while I-$Dcn^{-/-}$ exhibited decreased percent relaxation. Genotype and age significantly affected stress relaxation at 4% strain (Fig. 2B), while the interaction did not. I-$Dcn^{-/-}/Bgn^{-/-}$ displayed increased relaxation versus I-$Dcn^{-/-}$ at 300d, and increased relaxation versus WT and I-$Dcn^{-/-}$ at 570d. Stress relaxation at 5% strain (Fig. 2C) showed no significant differences between groups. Dynamic modulus (E*) and phase angle delta (δ) revealed no changes between genotypes, but age and the interaction was significant for I-$Dcn^{-/-}$ for E* and tan(δ) and for I-$Dcn^{-/-}/Bgn^{-/-}$ tan(δ) (Fig. 3). I-$Dcn^{-/-}$ E* was decreased at 570d vs 300d, while tan(δ) was increased (Fig. 3A-B). I-$Dcn^{-/-}/Bgn^{-/-}$ showed increased tan(δ) at 3% strain for 0.1-5 Hz, and 4% strain at 5 Hz (Fig. 3C). TEM analysis revealed that I-$Dcn^{-/-}$ and I-$Bgn^{-/-}$ had altered fibril diameters vs WT at 300d and 570d (Fig. 4). I-$Dcn^{-/-}/Bgn^{-/-}$ showed altered fibril diameter versus WT at 300d, but not 570d. Notably, I-$Dcn^{-/-}$ revealed increased fibril diameter heterogeneity, an increased maximum fibril diameter, and decreased minimum fibril diameter at 300d. At 570d, I-$Dcn^{-/-}$ fibril diameter was reduced versus WT in quartiles 2-4. Histology revealed no significant differences for cell shape or cellularity between any genotypes at 300d or 570d.

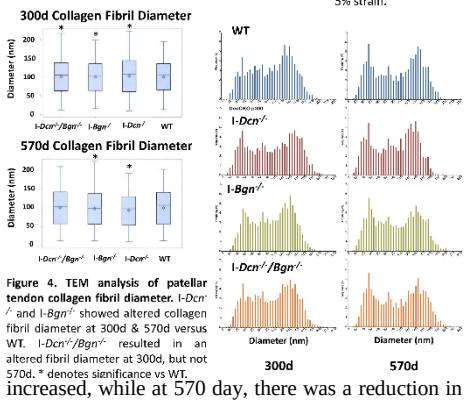

Figure 4. TEM analysis of patellar tendon collagen fibril diameter. I-$Dcn^{-/-}$ and I-$Bgn^{-/-}$ showed altered collagen fibril diameter at 300d & 570d versus WT. I-$Dcn^{-/-}/Bgn^{-/-}$ resulted in an altered fibril diameter at 300d, but not 570d. * denotes significance vs WT.

DISCUSSION: Supporting our hypothesis, the absence of Dcn resulted in a reduced impact from aging on tendon mechanics, including an increased midsubstance elastic modulus and decreased stress relaxation at 300 day vs WT. Additionally, at 300d, I-$Dcn^{-/-}$ had an improved dynamic modulus and phase angle vs I-$Dcn^{-/-}$ at 570d, indicating limitations to the extent that the absence of Dcn can improve tendon mechanics during aging. I-$Dcn^{-/-}$ also resulted in significant alterations in collagen fibril diameter compared to WT at both 300 and 570 day. At 300 day, the fibril diameter heterogeneity was increased, while at 570 day, there was a reduction in fibril diameter in the upper 75% of the distribution. Contrary to our hypothesis, the absence of both Dcn and Bgn did not result in an improved aging phenotype, with no changes in midsubstance or insertion modulus, and increased stress relaxation versus WT and I-$Dcn^{-/-}$. The absence of Bgn resulted in an altered fibril diameter distribution with no changes in mechanics. A role for both Dcn and Bgn was revealed in the maintenance of tendon structure at 300 and 570 days. These results support previous work examining the effects of Dcn during tendon aging, which showed no changes in mechanics between mature and aged Dcn knockout mice, while WT and Bgn knockout mice showed declining mechanics with age [3]. Further, reduced viscoelastic and elastic mechanics in I-$Dcn^{-/-}/Bgn^{-/-}$ versus WT at 150 day [5], provides evidence that I-$Dcn^{-/-}/Bgn^{-/-}$ has a distinct phenotype from both I-$Dcn^{-/-}$ and I-$Bgn^{-/-}$, when it was previously hypothesized that I-$Dcn^{-/-}/Bgn^{-/-}$ would result in a true Dcn knockout phenotype, without compensatory effects of Bgn. Overall, this study provides evidence for the detrimental effects of Dcn on tendon aging and the vital role of both Dcn and Bgn in regulating tendon structure.

SIGNIFICANCE: This study demonstrates that Dcn and Bgn play important differential roles in regulation of tendon structure during aging, with the absence of Dcn resulting in an improved tendon aging phenotype.

ACKNOWLEDGEMENTS: We acknowledge financial support from NIH/NIAMS R01AR068057, P30AR069619, and the NSF GRFP.

REFERENCES: [1] Buckwalter JA et al., 2003. *JBJS*, 85:748-758. [2] Schonherr E et al., 1995. *JBC*, 270:8877-83. [3] Dunkman AA et al., 2013. *Matrix Biol*., 32:3-13. [4] Beach ZM et al., 2018. ORS Paper No. 0237. [5] Robinson KA et al., 2017. *Matrix Biol*, 64:81-93. [6] Brodt MD et al., 1999. *JBMR*.

Effects of Pulsed Electromagnetic Field Therapy on Healing in a Rat Achilles Tendon Partial Width Injury Model Without Immobilization

Boorman-Padgett JF[1], Huegel J[1], Nuss CA[1], Minnig MCC[1], Raja HA[1], Kuntz AF[1], Waldorff EI[2], Zhang N[2], Ryaby JT[2], Soslowsky LJ[1]
[1]McKay Orthopaedic Research Laboratory, University of Pennsylvania, Philadelphia, PA, USA [2]Orthofix Inc., Lewisville, TX, USA

DISCLOSURES: Boorman-Padgett JF (N), Huegel J (N), Nuss CA (N), Minnig MCC (N), Raja HA (N), Kuntz AF (5-Orthofix, Inc), Waldorff EI (3A,4-Orthofix, Inc), Zhang N (3A- Orthofix, Inc), Ryaby JT (3A,4- Orthofix, Inc), Soslowsky LJ (5- Orthofix, Inc)

INTRODUCTION: Partial tears of the Achilles tendon are typically treated conservatively [1], often with various noninvasive therapies such as ultrasound. An FDA-approved Pulsed Electromagnetic Field (PEMF) therapy (Physio-Stim®, Orthofix Inc., Lewisville, TX, USA) has been shown to improve outcomes in tendon-to-bone rotator cuff healing in a rat model [2,3]. However, for partial Achilles tendon tears, the effects of PEMF therapy on in vivo joint function and ex vivo tendon fatigue properties remain inconclusive [4], as the use of postoperative plantarflexion immobilization confounded results in an earlier study. Therefore, the objective of this study was to quantify the effects of this FDA-approved PEMF therapy on joint and tendon level properties after a partial width, full thickness injury (partial tear) in the absence of limb immobilization. We hypothesized that PEMF treatment would improve Achilles tendon healing compared to a non-PEMF group.

METHODS: 144 adult male Sprague-Dawley rats (400-450g) were anesthetized with isoflurane, and underwent a unilateral, full thickness, partial width (1.5mm biopsy punch) Achilles tendon injury through the center of the tendon (IACUC approved). All animals were allowed cage activity throughout the study. Animals were placed into 3 groups (n=48/group): a control group receiving no PEMF treatment (non-PEMF), or a treatment group receiving either 1 or 3 hours of daily systemic PEMF (Physio-Stim®, 1HP and 3HP, respectively) therapy. Animals were sacrificed at 1, 3, or 6 weeks (n=16 per group per time point). All animals in the 6 week groups underwent longitudinal in vivo ambulatory assessment and passive ankle joint mechanics testing at 2, 4, and 6 weeks post-injury [5,6]. At sacrifice, the Achilles-calcaneus complex was dissected out (n=6 per group per time point) and processed for μCT scanning (21μm resolution) followed by decalcification and histological analysis. All other animals (n=10 per group per time point) were frozen at -20°C and thawed for dissection prior to tendon cross-sectional area measurement using a custom laser device and mechanical testing using a load controlled fatigue testing protocol [7]. For all measures, the two treatment groups (1HP and 3HP) were compared to the control (non-PEMF) group at each time point using two-tailed, t-tests after checking for normality. Bonferroni post-hoc corrections were applied for multiple comparisons and significance was set at $p<0.025$.

RESULTS: *Joint Range of Motion:* No differences were observed between the PEMF treatment groups and the non-PEMF group at any time point (data not shown). *Ambulatory Assessment:* Rats receiving 3 hours of PEMF treatment walked faster than non-PEMF animals 2 and 4 weeks post-injury. Rats receiving either 1 or 3 hours of PEMF treatment loaded their injured limbs faster than non-PEMF rats 2 weeks post-injury (Fig 1). *Histology:* Tendons receiving 3 hours of PEMF were less cellular than control non-PEMF tendons at 3 weeks, and exhibited greater collagen organization than control non-PEMF tendons at 6 weeks (data not shown). *Mechanical Testing:* No differences were observed between PEMF treated tendons and non-PEMF control tendons at any time point (Figs 2A & 2B). *μCT:* Heterotopic bone formation in the injured Achilles tendons was observed in all groups including the non-PEMF control, and at 6 weeks post-injury all scanned tendons contained bone. No differences were observed in bone volume or bone mineral density between the PEMF treated tendons and the non-PEMF control tendons at any time point (Fig 2C).

DISCUSSION: The aim of this study was to determine the effects of an FDA-approved, non-invasive PEMF treatment on rat Achilles tendons following partial injury without immobilization. We hypothesized that, in the absence of immobilization, PEMF treatment would result in improved healing compared to control tendons. However, no differences were observed in mechanical testing outcome measures generally associated with tendon function and healing. While some scattered differences were observed in ambulatory measures, the lack of corresponding changes in mechanical properties suggests that these are more likely the result of animal variations than they are the result of improved tendon function. While not different between treatment groups, the observed bone formation in this Achilles tendon injury model remains interesting and appeared to increase over time. It should be noted that heterotopic bone formation has been observed clinically as well. Ultimately, it appears that PEMF treatment does not improve tendon healing in this partial width, full thickness injury model without immobilization. Surprisingly, ambulatory and joint range of motion assessments detected very little loss of function following this injury model without immobilization. These results indicate that immobilization may be detrimental in this model. Additional comparisons are being performed to quantify this effect. Conversely, a previous study demonstrated that the same PEMF treatment had a positive effect on rat rotator cuff healing suggesting site-specific efficacy [3]. Overall, it is possible that this specific injury model is too conservative to measure potential therapeutic effects in the context of rapid baseline healing in these otherwise healthy Sprague-Dawley rats.

SIGNIFICANCE: This study shows that healing of a rat partial Achilles tendon injury is not improved by the use of PEMF therapy. Our previous study led to inconclusive results when immobilization was applied after injury [4]. This study provides clarity in the context of the earlier study and provides novel insight into the severity and complexity of this particular injury model.

REFERENCES: [1] Soroceanu A et al. J Bone Joint Surg Am. 2012 [2] Tucker JJ et al. J Orthop Res. 2016 [3] Huegel J et al. J Shoulder Elbow Surg. 2018 [4] Boorman-Padgett J et al. Trans ORS, 2018; 1454. [5] Sarver JJ et al. J Shoulder Elbow Surg. 2008 [6] Sarver JJ et al. J Biomech. 2010 [7] Pardes AM et al. Ann Biomed Eng. 2016.

ACKNOWLEDGEMENTS: Funding was provided by Orthofix, Inc. The authors wish to thank Stephanie Weiss, Mengcun Chen, and Adnan Cheema for their assistance with surgical procedures and Peter Chan for assistance with data processing.

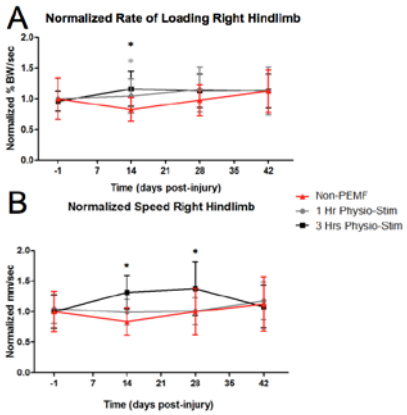

FIGURE 1: (A) Normalized rate of loading was increased in both PEMF treatment groups compared to non-PEMF animals 2 weeks after injury. (B) Normalized speed of the injured limb was increased in 3HP animals at 2 and 4 weeks after injury. Data are mean ± SD. Black asterisks indicate $p<0.025$ comparing 3HP to non-PEMF. Gray asterisks indicate $p<0.025$ comparing 1HP to non-PEMF.

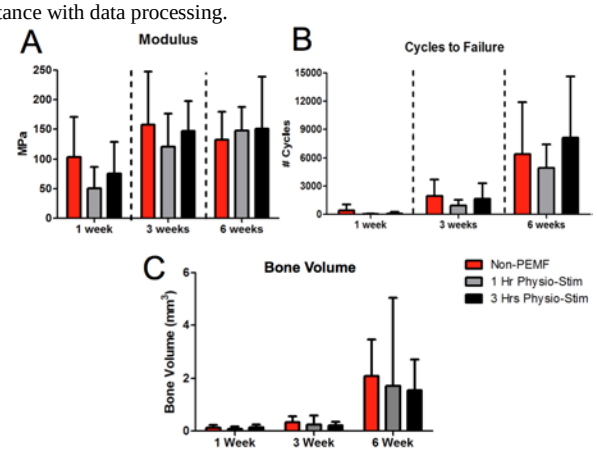

FIGURE 2: (A) Modulus values during mechanical testing were no different between PEMF treatment groups and control tendons. (B) Cycles to failure were no different between PEMF treatment groups and control tendons. (C) Bone volume was no different between treatment groups and control tendons but did appear to increase over time. Data are mean ± SD.

Gender Dependent Alterations in the Mechanical Response of Injured Collagen V Haploinsufficient Murine Tendons

Carlson JA[1], Johnston JM[1], Bonilla KA[1], Shetye SS[1], Nuss CA[1], Weiss SN[1], Rodriguez AB[1], Birk DB[2], Soslowsky LJ[1]
[1]McKay Orthopaedic Research Laboratory, University of Pennsylvania, Philadelphia, PA, [2] University of South Florida, Tampa, FL
Disclosures: Carlson JA(N), Johnston JM(N), Bonilla KA(N), Shetye SS(N), Nuss CA(N), Weiss SN(N), Rodriguez AB(N), Birk DB(N), Soslowsky LJ(N)

INTRODUCTION: Classic Ehlers-Danlos syndrome (*c*EDS) is most commonly characterized by haploinsufficiency in *COL5α1* with patients suffering from hyperextensible skin, joint instability and laxity. Collagen V is significantly upregulated following injury [1,2] and abnormal wound healing is associated with a diminished expression of collagen V [1,3]. Furthermore, estrogen in females is suggested to be associated with decreased collagen synthesis [4,5] and altered gene expression during repair [6]. However, the way gender-specific differences influence the healing response after injury and in the presence of collagen V deficiency has not yet been investigated. Therefore, the objectives of this study were to evaluate the mechanical response of injured patellar tendons over time in normal and *c*EDS mice, as well as differences between genders. We hypothesized that gender related differences in collagen V expression would result in an abnormal wound matrix in the injury response, contributing to the abnormal wound phenotype resulting in reduced mechanical properties of injured EDS tendons compared to normal tendons. In addition, the injury response in the female *c*EDS tendons will be inferior to that of male tendons due to these gender influences, resulting in greater mechanical properties of male tendons when compared to females.
METHODS: Adult male and female wild-type (WT) C57/BL6 and heterozygous (HET) ***Col5a1***$^{+/-}$ *c*EDS mice (n=120) at 120 days of age were used (IACUC approved). All mice underwent bilateral patellar tendon injury surgery as described [7] and were sacrificed 3 weeks or 6 weeks post-injury. *Mechanics.* The patella-patellar tendon-tibia complexes of all mice were dissected and prepared for mechanical testing [8]. Cross-sectional area was measured using a custom laser device [9]. Tendons were subjected to a viscoelastic testing protocol [8,10] consisting of: 1) preconditioning, 2) stress relaxation at strain levels of 2%, 3% and 4%, 3) a sinusoidal frequency sweep (10 cycles at 0.1, 1, 5, and 10 Hz) at each strain level, 4) return to gauge length, and 5) ramp to failure. Tendon length was measured at nominal load prior to test initiation. *Statistics.* Two-way ANOVAs with post-hoc Tukey tests were used to assess the effects of genotype (collagen V expression), gender, and their interaction on elastic and viscoelastic mechanical properties. Significance was set at $p \leq 0.05$ and trends at $p \leq 0.1$.
RESULTS: *Quasi-static:* WT male tendons had higher failure stress at 3w and 6w post-injury (PI), tissue modulus at 6w, and a trending increase in tissue modulus at 3w when compared to WT female tendons (Fig. 1A,B). WT male tendons also had higher failure loads and failure stiffness at 3w and 6w PI (Fig. 1C,D). HET males had higher failure stress and failure loads at 3w and 6w PI, and higher stiffness at 3w PI when compared to HET females (Fig. 1B,C,D). *Viscoelastic:* WT male tendons, when compared to WT female tendons 3w PI, had reduced dynamic moduli at 2% strain (.1 Hz and 1 Hz), with a trend towards a decrease at 2% strain, 10 Hz and 3% strain, 0.1 Hz, however no differences in HET mice between genders were seen at 3w PI (Fig. 2A,B). No WT differences in dynamic modulus were seen between genders at 6w PI (Fig. 2C,D). Additionally, WT males had a higher tan(δ) at 2% strain, .1 Hz at 3w and 6w PI when compared to WT females (data not shown). HET male and female tendons showed trending differences in dynamic modulus at 6w PI at lower frequencies at 3% and 4% strain (Fig. 2D, only 3% shown). The viscoelastic response of HET male tendons showed an increase in tan(δ) across all strains and frequencies (excluding 4%, 1 Hz and 4%, 10 Hz) 6w PI when compared to HET females (Fig. 3B, only 3% shown). Additionally, no differences were seen between genders or genotypes in cross sectional area (data not shown).
DISCUSSION: WT and HET male injured patellar tendons demonstrated higher material and structural properties compared to WT and HET female injured tendons, respectively, at both time points following injury. Reduction in collagen V had a greater effect on male tendon material response than female tendon response, which is consistent with previous findings in uninjured tendons [11]. When examining the viscoelastic response, although dynamic modulus was decreased in WT male tendons compared to WT female tendons 3w PI, these differences did not persist to 6w PI. Additionally, there were no gender differences in viscoelastic properties of HET tendons 3w PI, however, gender differences in these properties were seen in HET tendons 6w PI. This could be explained by a diminished late healing response in HET females compared to males, obscuring the increased effect of reduced collagen V on male tendons versus female tendons at the 6w time point. Male patellar tendon properties are more dependent on collagen V than female tendon properties and the reduction of collagen V affects the healing response of male and female tendons in differing capacities. Future work may include further characterizing the healing response through histological analysis to understand cellular differences that could explain these mechanical differences.
SIGNIFICANCE: This study demonstrates that gender-specific effects play an explicit role in tendon injury and healing and can influence the degree to which tendon properties of *c*EDS mice are affected.
REFERENCES: [1] Wenstrup RJ, et al. *J Biol Chem.* 2006. [2] Ainsworth SR, et al. *Clin Orthop Relat Res.* 1993. [3] Steinmann B, et al. *Connective Tissue and Its Heritable Disorders.* New York: Wiley-Liss; 2002. [4] Yu WD, et al. *Clin Orthop Relat Res.* 2001. [5] Kjaer M, et al. *J Anat.* 2006. [6] Hart DA, et al. *Clin Orthop Relat Res.* 1998. [7] Beason DP, et al. *J Biomech*, 2012. [8] Dunkman AA, et al. *Matrix Biol.* 2013. [9] Favata M, Bioengineering PhD Thesis Philadelphia: University of Pennsylvania. 2006. [10] Miller KS, et al. *J Biomech Eng.* 2012. [11] Carlson JA, et al. [Abstract] ORS 2018.
ACKNOWLEDGEMENTS: *This study was supported by NIH/NIAMS AR065995, AR044745 and the Penn Center for Musculoskeletal Disorders (AR069619).*

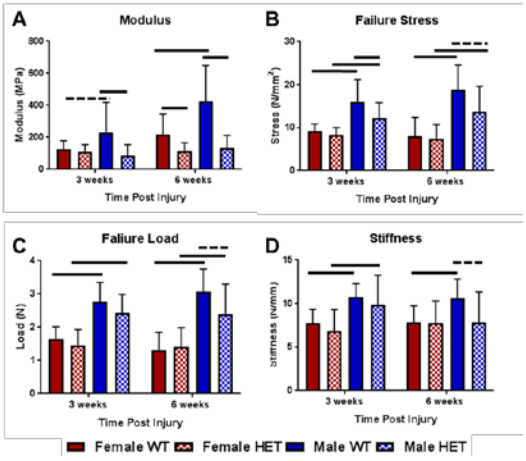

Figure 1. Material and structural and properties of female and male WT and HET patellar tendons. WT and HET male patellar tendons had increased moduli (A), failure stress (B), failure loads (C) and had increased stiffness (D) compared to female tendons.

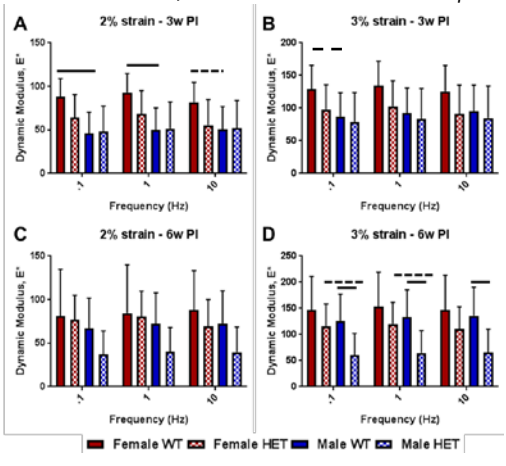

Figure 2. Dynamic moduli of female and male WT and HET patellar tendons. WT female patellar tendon dynamic moduli are increased across all frequencies at 2% strain, 3w PI (A), with no differences seen at 6w PI (C). Trending differences between genders were seen at lower frequencies at 3% strain, 6w PI (D).

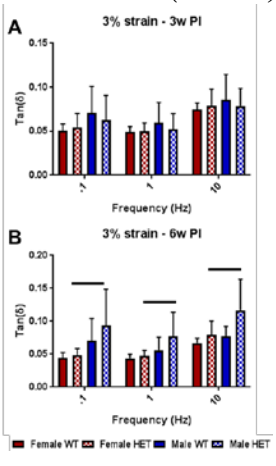

Figure 3. Tan(δ) of female and male WT and HET patellar tendons. HET male mice showed no differences in tan(δ) from HET female mice at 3w PI (A) but had increased tan(δ) measurements across all frequencies at 3% strain, 6w PI (B).

The Effects of Nicotine on Achilles Tendon Healing After Full Thickness Injury in a Rat Model

Adnan N. Cheema; Joseph Newton; James Boorman-Padgett; Stephanie Weiss; Courtney Nuss; Daniel J. Gittings; Daniel C. Farber; Louis J. Soslowsky
McKay Orthopaedic Research Laboratory, University of Pennsylvania, Philadelphia, PA

Disclosures: AC: None; JN: None; JBP: None; SW: None; CN: None; DJG: None; DCF: None; LJS: OrthoFix

INTRODUCTION: The consumption of nicotine products is rising [1] as e-cigarettes and similar products are marketed as safer alternatives to tobacco consumption. Nicotine has been shown to delay bone healing, accelerate vertebral disc degeneration, and hinder tendon to bone healing [1]. However, an understanding of its impact on intra-substance tendon healing is lacking. Therefore, the objective of this study is to investigate effects of nicotine on tendon healing after full thickness injury of the Achilles tendon in a rat. Functionally, we hypothesized that nicotine exposure would lead to a greater alteration in gait mechanics. Structurally, we hypothesized that nicotine would lead to decreased vascularity. Mechanically, we hypothesized that nicotine would lead to decreased maximum load, stiffness, cross sectional area, maximum stress, modulus, and stress relaxation.

METHODS: *Study Design:* 60 adult (10-13 week old) male Sprague-Dawley rats (IACUC approved) were randomized to receive either 0.9% saline (n=30) or 61mg/mL of nicotine (Nicotine, N3876, Sigma Aldrich, St. Louis, MO, n=30) through subcutaneously implanted osmotic pumps (2ML4; Alzet, Cupertino, CA). At 3 months, all rats underwent full thickness blunt transection of the left Achilles tendon [2]. Rats were sacrificed at 21 and 42 days post-injury. *Contrast Enhanced High Frequency Ultrasound*: Real-time ultrasound (MS250, VisualSonics, Toronto, ON) was used to assess the vascular status of the left Achilles tendons *in-vivo*. *Quantitative Ambulatory Assessment:* Ground reaction forces and temporal spatial parameters were measured using an instrumented walkway. *Passive Joint Mechanics:* Passive range of motion (ROM) and stiffness were measured using a custom device [3]. *Tendon Mechanics:* The Achilles tendon-bone complexes (n=10 per group, per time point) were subjected to a protocol of ten cycles of preconditioning, stress relaxation for 10 minutes at 5% strain, and ramp to failure at 0.1% strain/second [3,4]. *Statistics*: The Student's *t*-test was used to compare between groups. No comparisons across time were made. All data are presented as normalized to pre-injury values with mean ± standard deviation error bars. Normalized pre-injury value is represented as the dashed horizontal line.

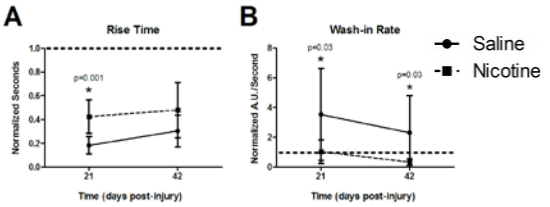

Figure 1. High frequency ultrasound data demonstrated (A) increased RT and (B) decreased WiR in the nicotine group, suggesting compromised vascular status. *A.U: Arbitrary Units*

RESULTS: *Contrast Enhanced High Frequency Ultrasound:* Rise Time (RT) and Wash-in Rate (WiR) were used as measures of contrast inflow. The nicotine group demonstrated an increase in RT (p=0.001) at 21 days and decreased WiR at both 21 (p=0.03) and 42 days (p=0.03) post-injury (Figure1). *Quantitative Ambulatory Assessment:* The nicotine group demonstrated decreased braking force (p<0.001) and decreased rate of loading (p=0.01) of the injured hindlimb (Figure 2). *Passive Joint Mechanics*: At 42 days, the nicotine group demonstrated decreased toe (p=0.003) and linear (p<0.001) region stiffness in dorsiflexion, decreased toe region stiffness (p=0.005) in plantarflexion, increased passive dorsiflexion ROM (p<0.001), increased passive plantar flexion ROM (p=0.0002), and increased total passive ROM (p<0.001) (not shown). *Tendon Mechanics:* At 21 days, the nicotine group showed increased maximum stress (p=0.02). At 42 days, the nicotine group demonstrated a decrease in cross sectional area (p<0.001), stiffness (p=0.01), maximum load to failure (p=0.02), and stress relaxation (p=0.02) (Figure 3).

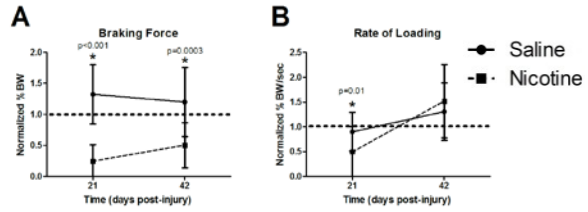

Figure 2. Quantitative ambulatory assessment revealed (A) decreased braking force and (B) decreased rate of loading in the nicotine group, demonstrating increased functional compromise and alteration of gait mechanics. *BW: body weight*.

DISCUSSION: The higher RT and lower WiR in the nicotine group reveal that nicotine inhibits vascular inflow at both early and late healing. The decreased braking force and rate of loading demonstrate that nicotine leads to greater functional impairment in the injured limb. Our data show that nicotine leads to an overall decrease in ankle stiffness and increased passive ROM. This is likely due to a decreased fibrotic healing response due to compromised vascular inflow. Nicotine leads to inferior elastic and viscoelastic biomechanical properties during late healing. The reduced stiffness may result in more elongation given the same load and result in greater functional impairment. The decreased load to failure may predispose patients to re-rupture of their tendons. Given that nicotine exposure already increases the risk of wound complications after surgical tendon repair, [5,6] re-rupture may limit future therapeutic options. Surprisingly, the maximum stress was increased in the nicotine group at 21 days, possibly due to physiological compensation during early healing. It may also partially explain why no biomechanical parameters were inferior in the nicotine group at that timepoint. Furthermore, since maximum stress is inversely related to CSA, the increased maximum stress in the nicotine rats may also be due to decreased CSA – a result of the decreased fibrotic healing response from vascular compromise.

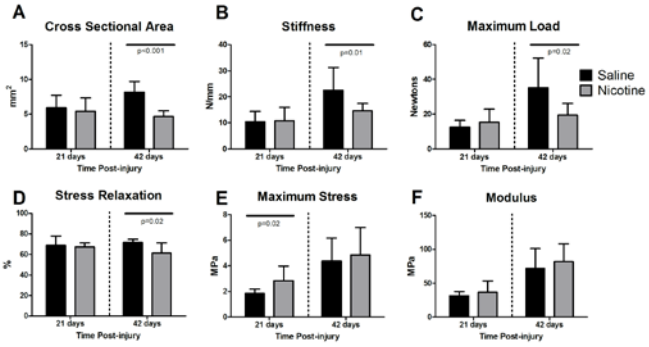

Figure 3. Biomechanical data showed (A) decreased CSA (B) decreased stiffness (C) decreased maximum load and (D) decreased stress relaxation in the nicotine group at 42 days. (E) Maximum stress was increased in the nicotine group at 21 days. (F) No differences in modulus were seen.

SIGNIFICANCE: This study demonstrates that nicotine leads to worse functional outcomes and inferior healing in Achilles tendons. The decreased vascularity in the nicotine group may suggest an underlying mechanism for inferior tendon healing. Patients should be counseled that using nicotine products such as tobacco, gums, patches, and e-cigarettes increase their risk of poor tendon healing and may predispose them to tendon re-rupture.

REFERENCES: [1] T. Hu et al. *Tob. Control*, 9:II60-3. 2000. [2] B. R. Freedman et al. *J. Biomech.* 47:2028–2034. 2014. [3] J. J. Sarver et al. *J. Shoulder Elb. Surg.* 17:108–113. 2008. [4] K. E. Reuther et al. *J. Orthop. Res.* 32:638–44. 2014. [5] D. P. Beason et al. *J. Shoulder Elb. Surg* 23: 867–872. 2014. [6] P. Silverstein. *Am. J. Med.* 93: 22–24. 1992.

ACKNOWLEDGEMENTS: The authors acknowledge Julianne Huegel, Harina Raja, Ashley Rodriguez, and Snehal Shetye for their contributions to this study. Funding was provided by the Orthopaedic Research and Education Foundation Grant (#17-011) and NIH/NIAMS supported Penn Center for Musculoskeletal Disorders Grant (P30AR069619).

Female Rat Supraspinatus Tendon Mechanical Properties Exhibit a Differential Response to Estrogen-Deficiency Depending on Reproductive History

Ashley K. Fung, Snehal S. Shetye, Chantal M. de Bakker, Yihan Li, X. Sherry Liu, Louis J. Soslowsky
McKay Orthopaedic Research Laboratory, University of Pennsylvania, Philadelphia, PA
afung@seas.upenn.edu

Disclosures: Ashley K. Fung (N), Snehal S. Shetye (N), Chantal M. de Bakker (N), Yihan Li (N), X. Sherry Liu (N), Louis J. Soslowsky (N)

INTRODUCTION: The prevalence of rotator cuff tears increases with age and postmenopausal women are at an even greater risk of developing full-thickness supraspinatus tendon tears [1]. Previous animal studies have supported these findings, demonstrating that an ovariectomy model of menopause led to reduced bone mineral density of the humeral head and decreased rotator cuff tendon strength [2,3]. Interestingly, recent preliminary data showed that prior to ovariectomy, reproductive female rats have inferior supraspinatus tendon and proximal humerus trabecular bone properties compared to virgin females; however, when subjected to ovariectomy, they experience a reduced rate of bone loss in the tibia compared to virgin females [4]. While these findings suggest a differential response in bone to estrogen-deficiency depending on reproductive history, how supraspinatus tendons are affected is unknown. Therefore, the objective of this study was to investigate the effect of reproductive history on female rat supraspinatus tendon mechanical properties following ovariectomy. We hypothesized that due to a dramatic decrease in estrogen levels and a high rate of early bone loss, ovariectomy will lead to a reduction in supraspinatus tendon mechanical properties.

METHODS: 58 female Sprague-Dawley rats (IACUC approved) were divided into virgin and reproductive groups. At age 4 months, reproductive rats underwent three cycles of reproduction, each consisting of a 3-week pregnancy, 3 weeks of lactation, and 3-6 weeks of post-weaning recovery. Virgin and reproductive rats underwent ovariectomy (OVX) surgery at 12 months of age and were sacrificed at 1 month (n=8/group), 3 months (n=8/group) or 6 months (n=5-7/group) post-OVX. Non-OVX, intact 13.5-month old virgin and reproductive female rats (n=7/group) were used as controls. Mechanics: Supraspinatus tendons were fine dissected and marked with stain lines for optical strain tracking. Cross-sectional area was measured using a custom laser device and humeri were secured in polymethyl methacrylate. Right supraspinatus tendons underwent quasi-static tensile testing, consisting of pre-conditioning (10 cycles from 0.5-1% strain), stress relaxation at 5% strain for 600s, dynamic frequency sweep at 5% strain (0.1-10Hz), and ramp to failure at rate of 0.3%/s. Statistics: Two-way ANOVAs were used to compare the effects of reproductive history and time after OVX with post-hoc Bonferroni corrections. Significance was set at $p \leq 0.05$ and trends at $p \leq 0.1$.

RESULTS: Cross-sectional area increased significantly in the reproductive group and trended towards increasing in the virgin group 1 month post-OVX (Fig 1A). By 6 months post-OVX, however, cross-sectional area was not different from control in either group. While stiffness trended towards increasing in the 3 month OVX reproductive group (Fig 1B), there were no changes in modulus in the reproductive groups. In contrast, modulus was significantly higher in the virgin non-OVX, control group compared to reproductive and significantly decreased in the virgin group at 1 and 3 months post-OVX (Fig 3C). At 6 months post-OVX, modulus in the virgin group increased compared to 1 month post-OVX and was significantly higher than the reproductive group. A similar trend was observed in the virgin group for dynamic modulus across all frequencies, where dynamic modulus was significantly lower at 1 month post-OVX and trended towards decreasing in the 3 month and 6 month groups, compared to control (Fig 1E). In the reproductive group, however, significant viscoelastic differences were observed at 1 month post-OVX. There was a significant increase in percent relaxation at 1 month post-OVX compared to control (Fig 1D), while dynamic modulus across all frequencies was decreased at 1 month compared to control, 3 month, and 6 month post-OVX groups (Fig 1E). Tan(δ) increased at 1 month post-OVX and was significantly higher than the virgin group at this time point (Fig 1F) with no differences at 3 months and 6 months.

DISCUSSION: This study investigated the effect of reproductive history on tendon properties following ovariectomy. Higher modulus in the virgin control group compared to the reproductive group was consistent with recent preliminary data for rats that had undergone 2 cycles of reproduction. Modulus had a significant interaction effect, where the virgin group experienced a reduction but the reproductive group exhibited no differences in response to OVX. Previous studies showed that rotator cuff tendon strength decreases with ovariectomy [2,3] and attributed these results to reduced structural integrity of the mineralized fibrocartilaginous insertion site. Other *in vitro* studies also found that estrogen plays a role in collagen synthesis and maintaining tissue elasticity [5,6]. Our findings suggest that, similar to bone, supraspinatus tendons of virgin and reproductive rats respond differently to estrogen deficiency. Interestingly, recent studies in bone uncovered several adaptation mechanisms, including redistribution of bone mass toward load-bearing compartments and increased bone mechano-sensitivity in reproductive rats, which may account for the protective effect of reproductive history on bone when subjected to estrogen deficiency [7]. Decreased viscoelastic parameters at 1 month post-OVX but recovery by 6 months in reproductive tendons suggest that additional tendon adaptation mechanisms developed during the course of reproduction may have altered the tendon response to estrogen deficiency later in life. Further studies are necessary to explore the mechanisms behind tendon adaptations in these models.

SIGNIFICANCE: This study highlights the importance of considering reproductive history during the diagnosis and treatment of rotator cuff injuries in post-menopausal women, particularly in the early stages of menopause where tendon properties were observed to change substantially.

REFERENCES: [1] Abate et al, 2014, *Menopause*. [2] Cadet et al, 2010, *J Orthop Res.* [3] Chen et al, 2015, *PLoS One*. [4] de Bakker et al, 2018, *J Bone Miner Res.* [5] Torricelli et al, 2013, *Age*. [6] Maman et al, 2016, *Connect Tissue Res*. [7] Li et al, 2018, *ORS Meeting*, 0695.

ACKNOWLEDGEMENTS: We thank H Zhao, WJ Tseng, and T Leahy for their assistance. This study was supported by NIH/NIAMS R03 AR065145, R01 AR071718, and the Penn Center for Musculoskeletal Disorders (P30 AR069619).

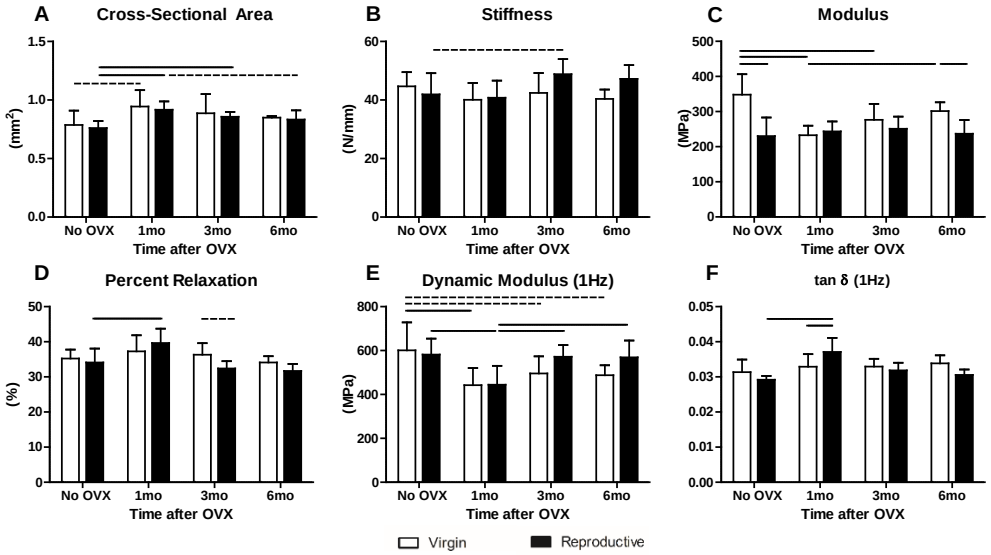

Figure 1: (A) Cross sectional area increased in the reproductive group at 1 month post-OVX but was not different from control by 6 months post-OVX. (B) Stiffness in the reproductive group trended towards increasing 3 months post-OVX, (C) but there were no differences in modulus in the reproductive rats. However, modulus significantly decreased in the virgin group at 1 and 3 months post-OVX. At 1 month post-OVX, the reproductive group exhibited (D) increased stress relaxation (E) decreased dynamic modulus and (F) increased tan(δ). Solid lines denote significance for $p \leq 0.05$ and dashed lines for trends $p \leq 0.1$.

Reproduction and Lactation Lead to Long-Term Changes in Supraspinatus Tendon and Humeral Trabecular Bone Properties in a Rat Model

Ashley K. Fung, Yihan Li, Thomas P. Leahy, Snehal S. Shetye, X. Sherry Liu, Louis J. Soslowsky
McKay Orthopaedic Research Laboratory, University of Pennsylvania, Philadelphia, PA
afung@seas.upenn.edu

Disclosures: Ashley K. Fung (N), Yihan Li (N), Thomas P. Leahy (N), Snehal S. Shetye (N), X. Sherry Liu (N), Louis J. Soslowsky (N)

INTRODUCTION: Physiological changes due to pregnancy increase the risk of developing musculoskeletal complications such as shoulder, lower back, and knee pain [1]. Altered levels of estrogen and relaxin during pregnancy increase knee joint and ligament laxity, compromising joint function, and these changes persist years after pregnancy [2]. Further, tibial and lumbar vertebral trabecular bone structure in reproductive female rats has been shown to be inferior compared to virgins but not different when compared to male, suggesting that reproduction and lactation induce bone loss that is not fully recovered post-weaning [3]. However, the long-term effects of reproduction on tendons and bones of the shoulder have not yet been studied. Therefore, the objective of this study was to evaluate the supraspinatus tendon mechanical response and humeral trabecular bone properties of male, virgin female, and reproductive female rats. We hypothesized that reproduction and lactation would induce long-term changes leading to inferior supraspinatus tendon properties and humeral trabecular bone microstructure in reproductive females as compared to virgin females.

METHODS: 20 Sprague-Dawley rats (IACUC approved) across three groups were used in this study: male (n=9), virgin female (n=6) and reproductive female (n=5). At age 6 months, reproductive female rats underwent two reproductive cycles, each consisting of a 3-week pregnancy, 3 weeks of lactation, and 6 weeks of post-weaning recovery. Rats were sacrificed at 12-14 months of age, and shoulders were harvested for supraspinatus tendon mechanical testing and trabecular bone analysis. Mechanics: Supraspinatus tendons were fine dissected and marked with stain lines for optical strain tracking. Cross-sectional area was measured using a custom laser device, and humeri were secured in polymethyl methacrylate. Right supraspinatus tendons underwent quasi-static tensile testing, consisting of pre-conditioning, stress relaxation at a 5% strain hold for 600s, a dynamic frequency sweep at 5% strain (0.1-10Hz), and ramp to failure at rate of 0.3%/s. Left supraspinatus tendons underwent fatigue testing, consisting of pre-conditioning and fatigue loading until failure at 2Hz between loads corresponding to 7% and 40% maximum stress, as determined from quasi-static testing. Fatigue parameters, including peak cyclic strain, secant modulus, tangent modulus, hysteresis, and laxity, were recorded at two breakpoints marking the ends of the primary (BP1) and secondary (BP2) phases of a triphasic fatigue life curve. Trabecular bone analysis: Left proximal humeri were scanned using μCT (10.5μm, μCT35, Scanco Medical). A 100-slice volume of interest proximal to the humeral growth plate was identified for trabecular bone microstructure analysis. Statistics: Comparisons across groups were made using one-way ANOVAs with Bonferroni post-hoc corrections. Significance was set at $p \leq 0.05$ and trends at $p \leq 0.1$.

RESULTS: Male tendons exhibited significantly higher stiffness compared to virgin and reproductive female tendons (Fig 1A). However, reproductive females had significantly lower modulus compared to virgin females but no difference compared to males (Fig 1B). Males had significantly lower dynamic modulus for all frequencies compared to both female groups (Fig 1C) but no difference in percent relaxation or tan(δ) (not shown). For fatigue properties at BP1, virgin females had significantly higher tangent and secant modulus compared to males and trended towards increasing compared to reproductive females (Fig 2A). However, there were no differences in secant or tangent modulus at BP2. No differences in hysteresis were observed at BP1, but reproductive females had significantly increased hysteresis compared to males at BP2 (Fig 2B). Cycles to failure and peak cyclic strain at BP1 was significantly higher in males compared to both female groups, and there were no differences in laxity at either breakpoint (not shown). Additionally, trabecular bone analysis revealed reduced bone volume fraction (BV/TV) and trabecular number (Tb.N) in reproductive females compared to virgin females but no difference compared to males (Fig 3A,B). Trabecular separation (Tb.Sp) in reproductive females was significantly increased compared to virgin females but trended towards a decrease when compared to males (Fig 3C). While trabecular thickness (Tb.Th) was significantly higher in males, there was no difference between female groups (not shown).

DISCUSSION: This study identified substantial differences in supraspinatus tendon and proximal humerus trabecular bone properties based on sex and reproductive history. Proximal humerus bone microstructure was superior in virgin females, consistent with previous findings in the tibia and vertebra. Previous research has linked ovariectomy to decreased failure stress of rotator cuff tendons and a less pronounced tidemark at the enthesis [4,5], and a similar mechanism may govern irrecoverable reproductive bone loss. Fatigue results also indicate that virgin and reproductive females experience a greater reduction in moduli and capacity to store energy, respectively, and together, these results suggest that females, regardless of reproductive history, may be more susceptible to early tendon degeneration. During pregnancy, hormonal fluctuations induce increased pelvic ligament laxity in preparation for parturition. Though the mechanisms are still unclear, several clinical studies have found sustained biomechanical changes in these ligaments despite a return to pre-pregnancy hormone levels [6,7]. Therefore, supraspinatus tendons following reproduction may be synergistically influenced by a direct effect of hormone changes and an indirect effect of bone loss near the insertion site. Shoulder pain after pregnancy has been associated with frequent breastfeeding that places added stress on the upper extremities. However, these findings suggest that biological changes during reproduction may inherently increase the risk for rotator cuff injury. Future studies will explore transient changes during pregnancy and investigate the mechanisms underlying long-term changes in tendon and bone properties following reproduction.

SIGNIFICANCE: This study identifies long-term changes in supraspinatus tendon and humeral trabecular bone properties that result following pregnancy and lactation, highlighting the importance of considering reproductive history in the diagnosis and treatment of shoulder injuries.

REFERENCES: [1] Koyasu et al, 2015, *Clin Exp Obstet Gynecol.* [2] Chu et al, 2018, *PM&R.* [3] de Bakker et al, 2018, *J Biomech.* [4] Cadet et al, 2010, *J Orthop Res.* [5] Chen et al, 2015, *PLoS One.* [6] Segal et al, 2013, *Am J Phys Med Rehabil.* [7] Damen et al, 2002, *Spine.*

ACKNOWLEDGEMENTS: This study was supported by NIH/NIAMS R03 AR065145, R01 AR071718, and the Penn Center for Musculoskeletal Disorders (P30 AR069619).

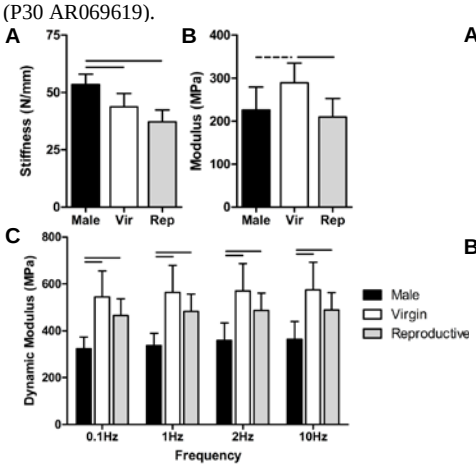

Figure 1: (A) Males had higher stiffness, while virgin females had increased (B) linear modulus and (C) dynamic modulus. Solid lines denote significance at $p \leq 0.05$ and dashed lines denote trends at $p \leq 0.1$

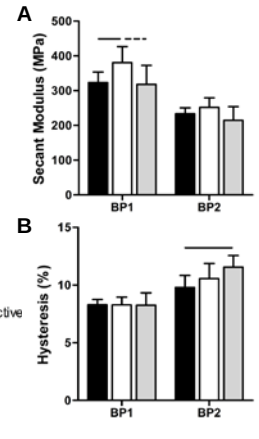

Figure 2: (A) Secant modulus was higher in the virgin group at BP1 and (B) reproductive females had increased hysteresis compared to males at BP2.

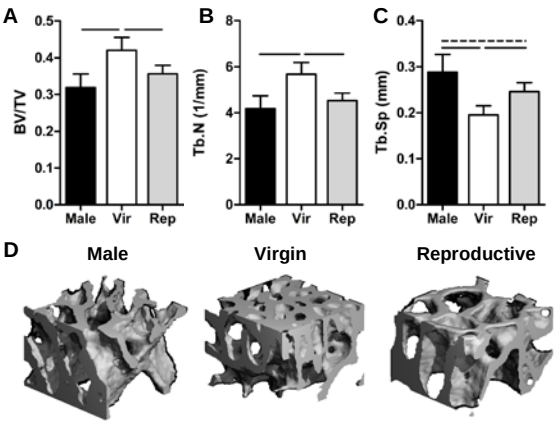

Figure 3: Virgin rats exhibited (A) higher bone volume fraction, (B) higher trabecular number, and (C) lower trabecular spacing compared to male and reproductive rats. Solid lines denote significance at $p \leq 0.05$ and dashed lines denote trends at $p \leq 0.1$. (D) Representative 3D humeral trabecular bone images

Quantitative Comparison of Three Rat Models of Achilles Tendon Injury: A Multidisciplinary Approach

Huegel J[1], Boorman-Padgett JF[1], Nuss CA[1], Minnig MCC[1], Kuntz AF[1], Waldorff EI[2], Zhang N[2], Ryaby JT[2], Soslowsky LJ[1]
[1]McKay Orthopaedic Research Laboratory, University of Pennsylvania, Philadelphia, PA [2]Orthofix Inc., Lewisville, TX

DISCLOSURES: Huegel J (N), Boorman-Padgett JF (N), Nuss CA (N), Minnig MCC (N), Kuntz AF (5-Orthofix, Inc), Waldorff EI (3A,4- Orthofix, Inc), Zhang N (3A- Orthofix, Inc), Ryaby JT (3A,4- Orthofix, Inc), Soslowsky LJ (5- Orthofix, Inc)

INTRODUCTION: The Achilles tendon, while the strongest and largest tendon in the body, is frequently injured. Even after surgical repair, patients risk re-rupture and can have long-term deficits in function, with the rate of return to pre-injury level of activity reported to be as low as 16% [1]. Animal models of tendon injury are essential for understanding physiological processes of tendon repair and for testing the effects of potential therapeutics [2]. We have adapted and utilized three rat models of Achilles tendon injury (complete, full-thickness tear with post-operative immobilization, partial tear with post-operative immobilization, and a partial tear without post-operative immobilization). However, comparisons of the effects of these injuries on tendon mechanics and ankle joint function have not previously been made. Therefore, the objective of this study was to quantitatively define and compare the effects and relative impact on tendon properties and ankle function of the three Achilles tendon injury models. We hypothesized that animals receiving a complete tear would have inferior mechanical properties and ankle function compared to those receiving a partial tear, and that immediate loading after a partial tear would improve post-operative mechanical properties and ankle function compared to immobilized tendons.

METHODS: 144 adult male Sprague-Dawley rats (400-450 g) were used (IACUC approved). Animals underwent either full-thickness, blunt complete transection and repair of the right Achilles tendon [3] (with one week of post-operative plantarflexion immobilization (CT+IM, n=48) or full-thickness, partial-width transection (1.5 mm biopsy punch in center of tendon) without repair [4] (with one week of post-operative plantarflexion, PT+IM, n=48, or without IM, PT-IM, n=48). Animals were sacrificed at 1, 3, or 6 weeks (n=16/group/time point). Animals in 6 week groups underwent longitudinal in vivo ambulatory and passive ankle joint mechanics assessments [3]. At sacrifice, the Achilles-calcaneus complex was dissected out (n=6/group/time point) and processed for histological analysis. All other animals (n=10/group/time point) were frozen at -20°C and thawed for dissection prior to cross-sectional area measurement using a custom laser device and mechanical testing using a load controlled fatigue testing protocol (including frequency sweeps at 0.1Hz, 1Hz, 5Hz, and 10Hz, and fatigue cycling from 5 to 35N cycles at2 Hz until failure) [3]. Post-test, tendons were scanned using μCT at a 21μm resolution to assess for presence of heterotopic ossification (HO) within the healing tendon. Statistical comparisons were made between the CT+IM and PT+IM group and between the PT+IM and PT-IM group at each time point. Comparisons for mechanics, functional assessments, collagen fiber organization, and μCT metrics were made using one way ANOVAs with Bonferroni post-hoc tests. Histological comparisons were made using Kruskal-Wallis tests.

RESULTS: *Mechanical properties*: At 3 and 6 weeks post-injury, cross-sectional area was larger for CT+IM tendons compared to PT+IM (Fig 1A). PT+IM modulus was significantly greater than CT+IM at 1 and 6 weeks, but was significantly lower than PT-IM at 3 weeks (Fig 1B). Similar differences were also seen in stiffness (Fig 1C). Dynamic frequency sweeps at 0.125% strain also determined similar differences in dynamic modulus at all tested frequencies (data not shown). PT-IM tendons withstood significantly more fatigue cycles before failing than PT+IM tendons at 3 and 6 weeks, and only PT-IM tendons were able to produce a reliable fatigue response at 3 weeks (Fig 1D,E). Tissue modulus (Fig 1E) and both secant and tangent stiffness (data not shown) measured during fatigue testing were greater in PT+IM tendons than in CT+IM at 6 weeks, but there was no difference between PT groups in these metrics at this time (Fig 1E). *Histological observations*: No differences were determined in cell number (cellularity), nuclear shape, or collagen organization. *μCT*: The presence of heterotopic ossification was observed in almost all samples in all groups at all time points (no differences between models, data not shown). Bone volume was significantly higher in CT+IM tendons than PT+IM tendons at six weeks (Fig 2A); however, this mineralized tissue had decreased tissue mineral density (Fig 2B). *Functional assessments*: Ankle joint stiffness and range of motion (ROM) through dorsiflexion were significantly altered in CT+IM and PT+IM groups (Fig 3A,B). Ankles from complete tendon tears were stiffer than both partial tear groups at 14 days post-injury, but by 6 weeks, were only stiffer than the PT-IM group (Fig 3A). In contrast, CT+IM and PT+IM groups had similarly diminished dorsiflexion ROM (~60% decrease) at 14 days (Fig 3B). PT+IM joints regained significantly more ROM by 6 weeks, while CT+IM joints did not recover (Fig 3B). Few differences existed in plantarflexion parameters (data not shown). CT+IM animals also had significantly slower rate of loading (Fig 3C) and longer stance time (data not shown) during ambulation than PT+IM, even though overall speed was increased at 6 weeks (data not shown).

DISCUSSION: This study investigated differences in ankle function, tendon mechanics, and HO in three different models of Achilles injury. All models were reproducible and had distinct effects on measured parameters. Injury severity (CT vs PT) had a drastic influence on tendon healing, with complete tear causing diminished ankle mobility and decreased tendon mechanics throughout post-injury time points compared to partial tears. Changes in loading rate and stance time of the injured limb indicate that CT animals are altering ambulation patterns more severely, which may be due to loss of function or increased pain [5]. CT tendons also contained significantly more HO than PT tendons. However, differences in bone density between groups suggest that the mechanisms of HO development or maturation may vary between models. One week of plantarflexion IM had a strong effect on animals receiving a partial-width injury. Most notably, tendons in the PT+IM group failed extremely early during fatigue cycling 3 weeks post-injury (113±85 cycles), prohibiting fatigue analysis. Surprisingly, a partial tear injury without immobilization had no effect on ankle range of motion through dorsiflexion at any time point, while PT+IM animals demonstrated diminished function at all post-injury time points. Together, these results indicate that even short-term immobilization may impair healing and increase ankle stiffness in partial Achilles tears in rats. Future studies will investigate long-term effects of these models.

SIGNIFICANCE: All three models of Achilles injury could be useful for tendon healing investigations, chosen based on the prospective applications of a potential therapeutic. This work also sheds light on the universal occurrence of heterotopic ossification after surgically-induced injury in a rat Achilles tendon, as well as the potentially detrimental effects of complete immobilization/unloading on partial Achilles tears.

REFERENCES: [1] Barfod KW et al. J Bone Joint Surg, 2014. [2] Hast MW et al. Bone Joint Res, 2014. [3] Freedman BR et al. J Orthop Res, 2016. [4] Boorman-Padgett J et al. Trans ORS, 2018; 1454. [5] Caro AC et al. J Am Assoc Lab Anim Sci, 2014.

ACKNOWLEDGEMENTS: Funding was provided by Orthofix, Inc and the Penn Center for Musculoskeletal Disorders (P30 AR069619). We thank Stephanie Weiss, Daniel Gittings, Adnan Cheema, and Mengcun Chen for help with surgies, and Peter Chan for help with μCT analysis.

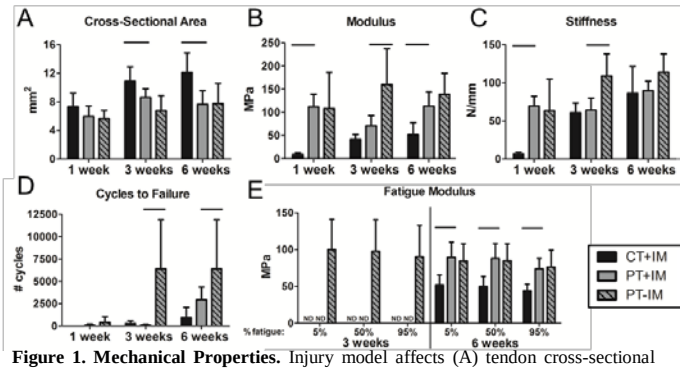

Figure 1. Mechanical Properties. Injury model affects (A) tendon cross-sectional area at 3 and 6 weeks; both injury mode and IM alter (B) tissue modulus and (C) tendon stiffness; immediate load bearing improves (D) cycles to failure at 3 and 6 weeks; and CT decreases (E) fatigue modulus at 6 weeks. ND: data was not able to be collected. Bars: p<0.025.

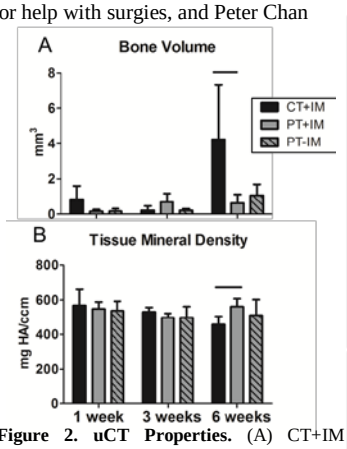

Figure 2. uCT Properties. (A) CT+IM showed (A) increased heterotopic bone volume but (B) decreased tissue mineral density at 6 weeks post-injury. Bars: p<0.025.

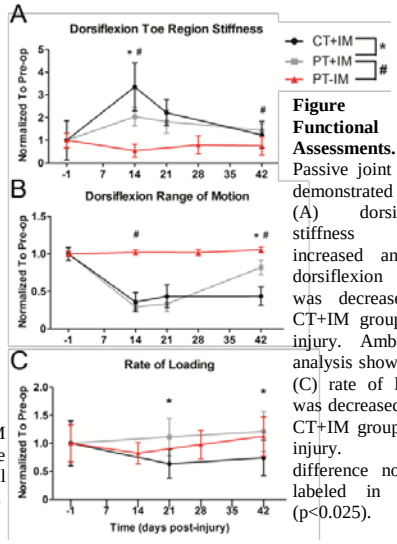

Figure 3. Functional Assessments. Passive joint testing demonstrated that (A) dorsiflexion stiffness was increased and (B) dorsiflexion ROM was decreased for CT+IM group post-injury. Ambulatory analysis showed that (C) rate of loading was decreased in the CT+IM group. post-injury. Sig difference notations labeled in legend (p<0.025).

Estrogen Deficiency and Intermittent Parathyroid Hormone Treatment Affect Regional Achilles Tendon Vessel Microarchitecture

Thomas P. Leahy[1], Benjamin R. Freedman[1,2,3], Wei-Ju Tseng[1], Snehal S. Shetye[1], X. Sherry Liu[1], Louis J. Soslowsky[2]
[1]McKay Orthopaedic Research Laboratory, University of Pennsylvania, PA; [2]John A. Paulson School of Engineering and Applied Sciences, Harvard University, Cambridge, MA; [3]Wyss Institute for Biologically Inspired Engineering, Cambridge, MA. tpleahy@seas.upenn.edu.

Disclosures: Thomas P. Leahy (N), Benjamin R. Freedman (N), Wei-Ju Tseng (N), Snehal S. Shetye (N), X. Sherry Liu (N), Louis J. Soslowsky (N)

INTRODUCTION: The Achilles tendon is frequently injured and vascularity has been implicated as a predictor of Achilles tendon injury and healing potential.[1] Estrogen deficiency and intermittent parathyroid hormone (iPTH) treatment have been shown to differentially affect tendon healing response.[2–7] In rat models of tendon injury, estrogen-deficiency results in decreased Achilles tendon mechanical properties,[3] while iPTH treatment increases fibrocartilage formation near the tendon insertion during the healing response.[2,6] Despite the significant effects that estrogen deficiency and iPTH treatment have shown on the tendon healing response in animal models, there has been little research investigating their effect on vascularity of the Achilles tendon. Therefore, the objective of this study was to evaluate how estrogen deficiency and iPTH treatment modulate vessel microarchitecture in a rat Achilles tendon. We hypothesized that estrogen deficiency, simulated by bilateral ovariectomy surgery (OVX), would cause a decrease in Achilles tendon vessel microarchitecture throughout the length of the tendon, while iPTH treatment would result in increased tendon vessel microarchitecture, particularly near the insertion.

METHODS: Study Design: At 3 months of age, female Sprague-Dawley rats (n=14) were divided into three groups (IACUC approved): VEH (n=4), iPTH (n=3), and OVX (n=7). The OVX rats received OVX surgeries at 3 months of age to simulate estrogen deficiency for 4 weeks. At 3.5 months of age, VEH and iPTH rats received subcutaneous injections of saline solution and iPTH (PTH 1-34, 60μg/kg/day, Bachem, Bubendorf, Switzerland), respectively for 5 days a week for 2 weeks. Vascular casting: At 4 months of age, a vascular casting procedure was performed by infusion of Microfil mixture (MV122, Flow Tech Inc., Carver, MA) in the rat vascular network as described.[8–10] Briefly, 50 mL heparin sodium solution, followed by 100 mL 0.9% normal saline and 50 mL 4% PFA into the abdominal aorta at 4.4 mL/min via a perfusion pump (Bio-Rad, Hercules, CA) while the animals were under anesthesia. A syringe was used to inject 5 mL Microfil® mixture with 3% catalyst at 0.3 mL/min and the animals were stored at 4°C for 24 hours to allow complete polymerization. Afterwards, both the left and right Achilles tendons were harvested and μCT-scanned at 3.5μm voxel size (μCT 35, Scanco Medical AG, Brüttisellen, Switzerland) at a 1.6 mm region of the tendon insertion proximal to the calcaneus and another 1.6 mm long region near the midsubstance of the tendon, 3.6 mm proximal from the end of the insertion region (Fig. 1). A custom MATLAB (Mathworks, Natick, MA) script was used to apply a local thresholding technique to segment casted blood vessels from surrounding soft tissue.[11] Finally, the vascular microarchitecture parameters vessel volume (VV), vessel number (Ves.N), vessel thickness (Ves.Th), vessel separation (Ves.Sp), and connectivity density (Conn.D) were evaluated. Analysis: Separate two-way ANOVAs for tendon region and treatment were performed comparing VEH and iPTH, and VEH and OVX. If the ANOVAs determined a significant effect ($p<0.05$), Student's t-tests were performed to compare region and/or treatment between specific groups. Significant interaction terms were also evaluated.

RESULTS: When comparing VEH-OVX, treatment was a significant factor in VV, Conn.D, Ves.N, and Ves.Th, while region was a significant factor in Ves.Th. There was a significant interaction term for Conn.D. Further, the midsubstance region of the OVX tendons had significantly lower VV, Ves.N, Ves.Th, and Conn.D, with a trend toward greater Ves.Sp relative to the VEH group (Fig. 2). In addition, Ves.Th was significantly greater in the midsubstance relative to the insertion in the VEH tendons. When comparing parameters for VEH-iPTH, there were significant effects of region on Ves.Th. However, there were no significant differences between the VEH and iPTH groups (Fig. 3).

DISCUSSION: We investigated the effects of estrogen deficiency and iPTH treatment on vascular microarchitecture in the rat Achilles tendon. As hypothesized, OVX resulted in reduced vascular microarchitecture of the Achilles tendon, with the most profound effects in the tendon midsubstance. While OVX has limited effects on rat Achilles tendon homeostatic function,[4] it has significant detrimental effects on Achilles tendon healing response, resulting in decreased mechanical properties, including reduced max stress and secant modulus during fatigue loading, as well as decreased joint range of motion, cell proliferation, and GAG content.[3,5] As vascularity has been implicated as a predictor of healing potential,[1] the reduced Achilles tendon vessel microarchitecture observed in this study provides a potential explanation for the reduced healing potential seen in estrogen-deficient Achilles tendons. Contrary to our hypothesis, iPTH treatment did not have a drastic effect on vessel microarchitecture. In previous studies in bone, iPTH treatment did not result in osteoangiogenesis but rather relocated the vascular structure closer to the sites of new bone formation, thereby providing a favorable microenvironment for growth.[12] It may be possible that a similar effect happens in tendon, though it is also possible that the increased fibrocartilage formation in the tendon insertion observed previously is specific to the healing response.[2,6] Further studies should evaluate the effects of estrogen deficiency and iPTH treatment on vascular microarchitecture in an Achilles rupture model.

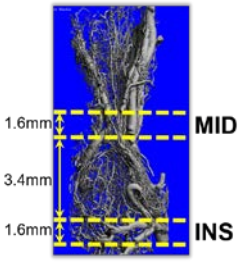

Figure 1. Achilles tendon vascularity, denoting insertion and midsubstance regions.

SIGNIFICANCE: This study highlights estrogen deficiency and iPTH treatment effects on vascular microarchitecture in the rat Achilles tendon. The decrease in tendon vascular microarchitecture in the estrogen-deficient rats could be a possible explanation for the reduced healing potential with estrogen deficiency.

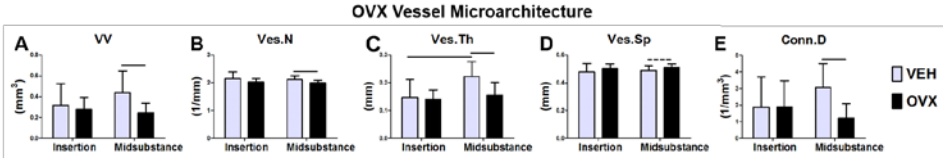

Figure 2. OVX vessel microarchitecture comparisons to the VEH group for VV (A), Ves.N (B), Ves.Th (C), Ves.Sp (D), and Conn.D (E). OVX shows detrimental effects on Achilles tendon vascular microarchitecture, particularly in the midsubstance region.

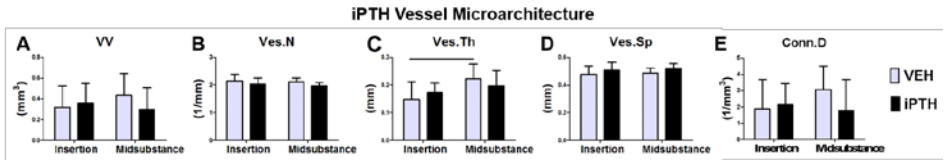

Figure 3. iPTH vessel microarchitecture comparisons to the VEH group for VV (A), Ves.N (B), Ves.Th (C), Ves.Sp (D), and Conn.D (E). iPTH treatment shows no differences compared to the VEH group except for eliminating the difference in Ves.Th between the insertion and midsubstance.

REFERENCES: [1] Theobald P et al., Injury, 2005. [2] Hettrich CM et al., J Orthop Res, 2012. [3] Fryhofer GW et al., J Appl Phsiol, 2016. [4] Pardes AM et al., Ann Biomed Eng, 2016. [5] Circi E et al., Int Orthop, 2009. [6] Duchman KR et al., J Shoulder Elbow Surg, 2016. [7] Lee DJ et al., J Orthop Res, 2015. [8] Wang Y et al., J Clin Invest, 2007. [9] Razavi H et al., Microvasc Res, 2012. [10] Duvall CL et al., Am J Physiol Heart Circ Physiol, 2004. [11] Waarsing JH et al., J Bone Miner Res, 2004. [12] Prisby R et al., J Bone Miner Res, 2011.

ACKNOWLEDGEMENTS: This study was supported by the Penn Center for Musculoskeletal Disorders (NIH/NIAMS P30 AR069619).

Collagen VI Plays an Important Role in FDL Tendon Mechanics that is Distinct from the Role of Biglycan

Ryan J Leiphart[1], Snehal S Shetye[1], Hai Pham[2], Stephanie N Weiss[1], Marian F Young[2], Louis J Soslowsky[1]
[1]McKay Orthopedic Research Laboratory, University of Pennsylvania, Philadelphia, PA
[2]National Institute of Dental and Craniofacial Research, National Institutes of Health, Bethesda, MD

Disclosures: RJ Leiphart (N), SS Shetye (N), H Pham (N), SN Weiss (N), MF Young (N), LJ Soslowsky (N)

INTRODUCTION: While tendons are largely composed of tension-bearing collagen I fibers, other lower abundance matrix proteins with lesser known functions are also present. For example, collagen VI is a nonfibrillar collagen that enriches the pericellular matrix (PCM), and biglycan is a small, leucine-rich proteoglycan that regulates fibrillogenesis [1,2]. Deficiency in either collagen VI or biglycan is known to impact tendon mechanics [3,4]. While collagen VI and biglycan are known to interact, their interactions in native tendon, and the impact on tendon mechanics, remain unknown [5]. Therefore, the objective of this study was to determine how the roles of collagen VI, biglycan, or interactions involving both molecules affect FDL tendon mechanics. We hypothesized that knockout of collagen VI would reduce FDL tendon mechanical properties more than knockout of biglycan, while blocking interactions by knocking out both molecules would lead to a larger reduction in these properties than the reduction seen in either knockout alone.

METHODS: *Animals and Dissection*: 2 month old male wild-type (WT) (n=16), *Col6a2*$^{-/-}$ (n=11), *Bgn*$^{-/0}$ (n=12), and *Col6a2*$^{-/-}$/*Bgn*$^{-/0}$ (n=13) mice were used in this study (IACUC approved). FDL tendons were dissected from the left hind limb. The tendon sheath was fine dissected off the tendon. Tendon cross-sectional area (CSA) was measured with a custom laser device, and stain lines were applied for optical tracking [6]. *Mechanical Testing*: The FDL tendon was gripped with sandpaper, leaving a 5mm gauge length. The testing protocol consisted of 10 cycles of preconditioning between 0.01-0.02N at 1Hz, a 5 minute hold, a 5% stress relaxation for 10 minutes, a 1 minute hold, and a ramp to failure at 0.5% strain/s. Stress relaxation, stiffness, max load, modulus, and max stress were computed. Dynamic collagen fiber realignment was measured throughout the ramp-to-failure test using a crossed polarizer setup [7]. *Statistics*: For mechanical properties, a one-way ANOVA with Bonferroni post-hoc tests was used to compare across genotypes. For fiber alignment data, a two-way ANOVA with Tukey correction for multiple comparisons was used to compare across genotype and strain. Significance was set at $p<0.05$, and trends were set at $p<0.10$.

RESULTS: WT tendons had larger CSA than tendons from all knockout genotypes (Fig 1A). *Bgn*$^{-/0}$ tendons had larger CSA than *Col6a2*$^{-/-}$ and *Col6a2*$^{-/-}$/*Bgn*$^{-/0}$ tendons. WT tendons were stiffer and had higher max loads than tendons from all knockout genotypes (Fig 1B,C). *Bgn*$^{-/0}$ tendons were stiffer than *Col6a2*$^{-/-}$ and *Col6a2*$^{-/-}$/*Bgn*$^{-/0}$ tendons. *Bgn*$^{-/0}$ and *Col6a2*$^{-/-}$ tendons had higher max loads than *Col6a2*$^{-/-}$/*Bgn*$^{-/0}$ tendons. WT and *Bgn*$^{-/0}$ tendons exhibited a larger percent relaxation than *Col6a2*$^{-/-}$ and *Col6a2*$^{-/-}$/*Bgn*$^{-/0}$ tendons (Fig 2A). No differences in moduli were observed between groups (Fig 2B). *Col6a2*$^{-/-}$ and *Col6a2*$^{-/-}$/*Bgn*$^{-/0}$ tendons had higher max stresses than WT and *Bgn*$^{-/0}$ tendons (Fig 2C). During the ramp to failure, WT tendons realigned between 3% and 5% strain (Fig 3). Bgn$^{-/0}$ tendons realigned between 5% and 7% strain. *Col6a2*$^{-/-}$ and *Col6a2*$^{-/-}$/*Bgn*$^{-/0}$ tendons realigned between 1% and 3% strain. At 3% and 5% strain, *Col6a2*$^{-/-}$ and *Col6a2*$^{-/-}$/*Bgn*$^{-/0}$ tendons were more aligned, and WT tendons trended towards more alignment, compared to *Bgn*$^{-/0}$ tendons.

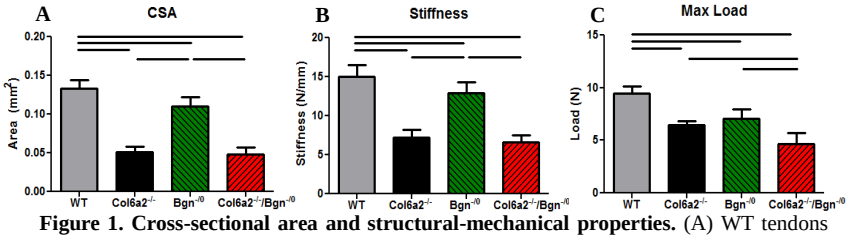

Figure 1. Cross-sectional area and structural-mechanical properties. (A) WT tendons had a larger CSA than all knockout genotypes. (B) WT tendons were stiffer than all knockout genotypes. (C) WT tendons had a higher max load than all knockout genotypes. Bars indicate $p<0.05$.

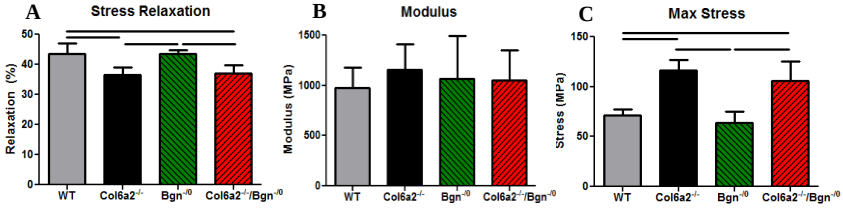

Figure 2. Viscoelastic and material properties. (A) WT and *Bgn*$^{-/0}$ tendons exhibited more stress relaxation than either collagen VI knockout models. (B) No differences in moduli were observed between genotypes. (C) Both collagen VI knockout tendons had higher max stresses than WT and *Bgn*$^{-/0}$ tendons. Bars indicate $p<0.05$.

DISCUSSION: While biglycan deficiency led to some decreases in FDL structural-mechanical properties (stiffness, max load), collagen VI deficiency led to larger reductions in structural-mechanical and viscoelastic properties. Knockout of biglycan or collagen VI led to smaller, less stiff, and weaker tendons than WT, but *Bgn*$^{-/0}$ tendons were larger and stiffer than *Col6a2*$^{-/-}$ tendons. Biglycan deficiency led to delayed fiber realignment compared to WT tendons, while collagen VI deficiency led to earlier realignment. *Col6a2*$^{-/-}$ tendons were less viscoelastic than *Bgn*$^{-/0}$ and WT tendons. These results agree with our hypothesis that collagen VI deficiency would reduce tendon mechanical properties more than biglycan deficiency. These mechanical and viscoelastic changes did not correspond to similar differences in material properties (modulus, max stress). There were no differences in moduli between WT, *Bgn*$^{-/0}$, and *Col6a2*$^{-/-}$ tendons, and *Col6a2*$^{-/-}$ tendons had higher max stresses than WT and *Bgn*$^{-/0}$ tendons. Our hypothesis that either knockout would reduce material properties was rejected. The different responses between the structural-mechanical and material properties could be due to smaller CSA in knockout tendons. Contrary to our hypothesis, knocking out both molecules did not amplify the differences seen in the *Col6a2*$^{-/-}$ mice. *Col6a2*$^{-/-}$ and *Col6a2*$^{-/-}$/*Bgn*$^{-/0}$ tendons had similar CSA, stiffness, moduli, max stress, stress relaxation, and fiber realignment. Due to its proximity to tendon cells within the tendon PCM, collagen VI is likely an important regulator of tendon cell behavior. The results of this study suggest that collagen VI regulation is so robust that it dominates any biglycan regulatory effects. This study is limited in that the knockouts are global. Changes in neighboring tissues, such as muscle and bone, may confound the effects of these knockout models on tendon properties specifically. Future studies will aim to elucidate the mechanisms by which collagen VI and biglycan regulate tendon properties. Another surprising finding in this study is that the biglycan knockout results differ from those of a previous study, which may be due to differences in CSA measurement [4]. The laser device used in the present study is more precise than the previous approach [6]. Overall, this study demonstrates that collagen VI and biglycan play distinct roles in regulating tendon mechanics and that collagen VI has a larger impact on mechanical properties.

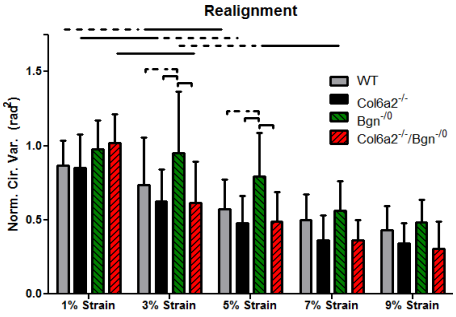

Figure 3. Fiber realignment during ramp to failure. Compared to WT tendons, *Bgn*$^{-/0}$ tendons realigned later. *Col6a2*$^{-/-}$ and *Col6a2*$^{-/-}$/ *Bgn*$^{-/0}$ tendons realigned earlier. A lower circular variance value indicates more alignment. Smooth bars compare adjacent strain values. Notched bars compare between genotypes. Solid bars indicate $p<0.05$, and dashed bars indicate $p<0.10$.

SIGNIFICANCE: This study reveals unique roles of collagen VI and biglycan in tendon mechanics and demonstrates that collagen VI has a larger impact on mechanical properties. These results provide further understanding of the role of lower abundance matrix proteins in tendon function.

REFERENCES: [1] Ritty TM et al. *Structure*. 2003. [2] Ameye L et al. *FASEB J*. 2002. [3] Izu Y et al. *Matrix Biol*. 2011. [4] Robinson PS et al. *J Biomech Eng*. 2005. [5] Wiberg C et al. *J Biol Chem*. 2002. [6] Favata, M *University of Pennsylvania*. 2006. [7] Lake SP et al. *J Orthop Res*. 2009.

ACKNOWLEDGEMENTS: This work was supported by the NIH (P30AR069619, T32AR007132), the Intramural Research Program of the NIH, NIDCR (Z01DE000379), and the NSF GRFP.

Anterior Drawer Tests to Quantify the Stability of the Murine Knee

Snehal S. Shetye[1], Yusuke Hagiwara[2], Ashley B. Rodriguez[1], Miltiadis Zgonis[1], Andrew F. Kuntz[1], Nathaniel A. Dyment[1]
[1]University of Pennsylvania, Philadelphia, PA, [2]Nippon Medical School Hospital, Tokyo, Japan
shetye@pennmedicine.upenn.edu

Disclosures: SS Shetye (N), Y Hagiwara (N), AB Rodriguez (N), M Zgonis (N), AF Kuntz (N), NA Dyment (N).

INTRODUCTION: Murine models of altered knee loading are routinely used to study the pathogenesis of post-traumatic osteoarthritis (PTOA). Such models include anterior cruciate ligament (ACL) transection, ACL rupture, or destabilization of the medial meniscus (DMM) [1]. These surgeries are typically applied to transgenic mice (i.e., knockout models) to better understand the role of certain genes and pathways in the pathogenesis. However, many of these studies have not investigated the stability of the knee following these surgical interventions and genetic treatments. We aimed to address this gap in knowledge by developing two methods to test the anterior-posterior stability of the knee following ACL injury and/or reconstruction.

METHODS: Experimental Design. All animals and procedures were approved by UPenn's IACUC. Adult mice were assigned to two methods of measuring knee stability through load-control anterior-posterior drawer tests. *Faxitron group*: Mice were assigned to intact (n=9), ACL transection (ACLT, n=9), and ACL reconstruction (ACLR, n=8) groups. The ACLT and ACLR mice were assessed at 4 weeks post-surgery. *Instron group*: Anterior-posterior drawer were applied to intact limbs, then the ACL was transected using a 25G needle and the test was conducted again on the same specimen (n=3). ACL transection and reconstruction procedure. All surgical procedures were performed under a microscope. One knee joint of each mouse was subjected to ACLT and/or ACLR. The contralateral knee joint served as an intact control. Following general anesthesia and aseptic preparation of the surgical site, tail tendon fascicles (3-4 cm long) were harvested from the proximal tail. The tendon bundles were maintained in PBS and sutured at both ends with 7-0 nylon. Surgical transection of the ACL was achieved via mid-vastus incision and subsequently transecting the ACL with a 27G needle [2]. After confirmation of significant anterior drawer and intact PCL, 27G needles were used to drill tunnels originating at the ACL femoral and tibial footprints through the femur and tibia. The tail tendon bundle was folded over and passed through the tunnels and secured to the upper lateral femoral epicondyle with a stainless steel washer endobutton. External tibial fixation was achieved by tensioning the graft with the knee in extension and tying the tail tendon bundle to an additional endobutton. *Faxitron drawer test*: Following sacrifice and isolation of hindlimbs, the tibia was fixed to a styrofoam block with 27G needle and then anchored to imaging platform of Faxitron LX-60. A needle was passed through the femur and suture was anchored to the needle then passed over a pulley at the edge of the platform and attached to a 10g weight. The weight was applied in the anterior direction, an x-ray was acquired, then the weight was applied in the posterior direction followed by another x-ray acquisition. X-rays were overlaid and the displacement of the anterior surface of the femur between anterior and posterior images was measured and then normalized to the anterior-posterior width of the tibial plateau. *Instron drawer test*: Following sacrifice, left hindlimbs were isolated and all extraneous soft tissue removed under a dissection microscope. All capsule ligaments, including the cruciates and collaterals, along with the menisci were left intact. The distal half of each tibia was potted in an acrylic tube using PMMA. This construct was then loaded onto a material testing machine. The potted tibial end was fixed in a custom fixture that allowed for adjustment of tibial plateau angle. The distal end of the femur was lowered into another acrylic tube affixed to a custom fixture that could control knee flexion by rotating the femur around the joint center of rotation (Fig. 2). The knee joint was tested for anterior and posterior stability by cyclic loading between ±0.4N for 10 cycles and the 10th cycle was used to quantify stability. *Stats*. Mann-Whitney U tests were conducted ($p<0.017$ for Faxitron test to account for multiple comparison and $p<0.05$ for Instron test)

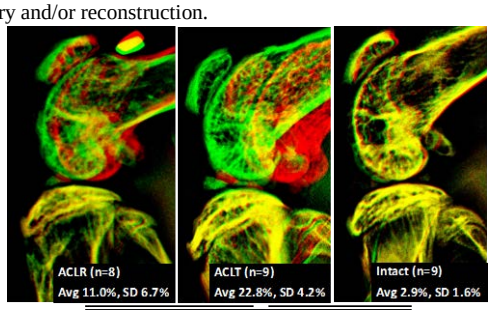

Figure 1: ACLT displays significantly greater anterior-posterior translation compared to ACLR or intact controls via Faxitron method. Bars at bottom indicate $p < 0.017$.

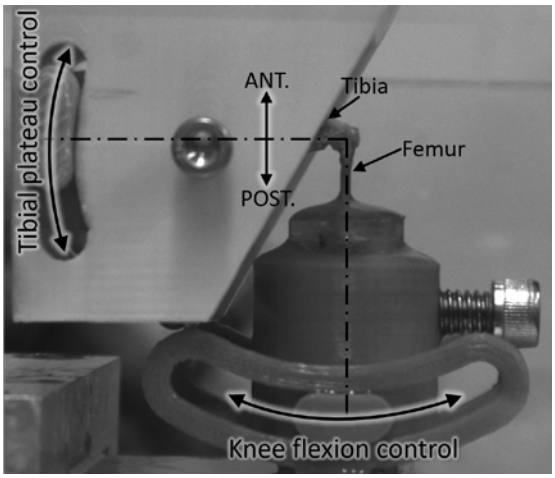

Figure 2: Instron setup to quantify the stability of murine knee. The custom fixtures allow for fine adjustment of knee flexion and orientation of the tibial plateau.

RESULTS: *Faxitron test*: Femurs from the ACLT samples translated a distance that equated to 22.8±6.7% of the tibial plateau width, which was 8X greater than intact controls (2.9±1.6%) (Fig. 1). The ACL reconstruction procedure restored over 50% of the stability lost by ACLT (11.0±6.7%) ($p < 0.05$). *Instron test:* ACLT samples experienced 104.1±63.5% more anterior translation when compared with intact controls ($p<0.05$, Fig. 3).

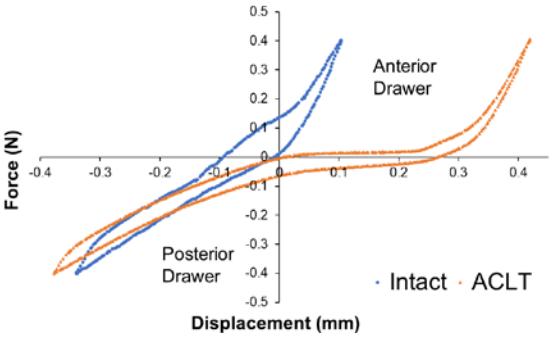

Figure 3: Representative graph depicting the loss of anterior stability after transection of the ACL. Lower left quadrant demonstrates that knee posterior stability remains intact.

DISCUSSION: In order to better understand the genetic/biologic mechanisms that regulate PTOA pathogenesis in these murine models, we need a better understanding of the mechanical stability of the knee joint following these treatments. These two test methods presented here offer researchers practical options to measure the anterior-posterior stability of the murine knee joint within PTOA models. Both methods are sufficient to detect statistical differences in displacement following an applied load. The Instron method requires specialized grips to adjust the tibia and femur correctly, making it more complex. However, viscoelastic properties can be measured with the Instron method unlike the Faxitron method. The observed percent change in displacement fell well within previous reports for anterior drawer tests in ACL-deficient human knees [3, 4].

SIGNIFICANCE/CLINICAL RELEVANCE: As murine PTOA models become more prevalent, it is imperative that the mechanical stability of the joint be assessed in these models, especially surgical models that lead to mechanical instability of the knee. These two test methods provide researchers with new protocols to assess anterior-posterior stability of the knee joint and show that ACLT results in murine knees correlate with previous studies in human knees.

REFERENCES: [1] Blaker CL et al., *J Orthop Res*, 2017 *(*35)424–439 [2] Dyment et al., *Osteoarthritis Cartilage*, 2015 (23)1-11 [3] Furman W. et al., *JBJS* 1976 (58)179-185 [4] Hsieh HH et al., *JBJS* 1976 (58)87-93

ACKNOWLEDGEMENTS: Study supported in part by the Penn Center for Musculoskeletal Disorders (P30 AR069619) and NIH (R00 AR067283).

Localized Delivery of Ibuprofen via a Bilayer Delivery System (BiLDS) for Supraspinatus Tendon Healing in a Rat Model

Brittany L. Taylor[1,2], Dong Hwa Kim[1,2], Julianne Huegel[1,2], Sophie J. Burkholder[1], Stephanie N. Weiss[1,2], Courtney A. Nuss[1,2], Harina A. Raja[1,2], Louis J. Soslowsky[1,2], Robert L. Mauck[1,2], Andrew F. Kuntz[1,2], Joseph Bernstein[1,2]
[1]Philadelphia VA Medical Center, Philadelphia, PA, [2]McKay Orthopaedic Research Laboratory, University of Pennsylvania, Philadelphia, PA,
brtay@pennmedicine.upenn.edu

Disclosures: B. L. Taylor (N), D.H. Kim (N), J. Huegel (N), S. Burkholder (N), S. N. Weiss (N), C. A. Nuss (N), H. A. Raja (N), L. J. Soslowsky (5; Orthofix), R. L. Mauck (8; JOR Spine), A. F. Kuntz (N), J. Bernstein (7B; CORR)

INTRODUCTION: The high prevalence of tendon re-tear following rotator cuff repair motivates the development of new therapeutics to promote improved tendon healing. Controlled delivery of non-steroidal anti-inflammatory drugs (NSAIDs) to the repair site via an implanted scaffold is a promising option for modulating inflammation in the healing environment. Previous work confirmed the *in vitro* sustained release of ibuprofen (IBP) from Labrafil-modified poly(lactic-co-glycolic) acid (PLGA) microspheres within sintered poly(ε-caprolactone) (PCL) electrospun scaffolds [1]. Biocompatibility of this bilayer delivery system (BiLDS) was also demonstrated with primary rat bicep and Achilles tenocytes *in vitro* [1, 2]. However, the effect of these IBP-releasing BiLDS on tendon healing *in vivo* is unknown. Therefore, the objective of this study was to investigate the effects of sustained release of IBP from BiLDS implanted at the repair site in a rat supraspinatus injury and repair model. We hypothesized that the controlled release of IBP from BiLDS would improve tendon healing by decreasing the expression of pro-inflammatory cytokines, thus improving tendon remodeling and mechanics.

METHODS: *BiLDS Fabrication*: PLGA microspheres with 300µL of Labrafil® M1944CS oil and with or without 30mg/mL of IBP were created as described [1]. 170µg of the microspheres, with or without IBP, were entrapped between two sintered 3x5mm scaffolds to generate BiLDS_IBP or BiLDS implants, respectively. Based on *in vitro* release studies, we predicted that the100µm thick BiLDS would deliver approximately 270µg of IBP to the injury site over 8 weeks. *BiLDS In Vivo Implantation*: 90 adult male Sprague-Dawley rats (400-450g) underwent bilateral supraspinatus detachment and repair (IACUC approved) [3]. Animals were randomly divided into groups receiving no scaffold (No_BiLDS), BiLDS with empty microspheres (BiLDS), and BiLDS with IBP-loaded microspheres (BiLDS_IBP) (n=30/group). BiLDS were secured proximally to the tendon via sutures and distally to the bone tunnel drilled through the greater tuberosity. Animals were sacrificed at 1, 4, and 8 weeks post-surgery. The right supraspinatus tendons and blood serum were collected at the time of sacrifice for biological assessment. *Biological Assessment:* Sagittal sections were stained with H&E, imaged at 20X and graded for cell shape and cellularity (n=6/group/timepoint). RNA was extracted from tendons harvested one week post-surgery (n=6/group) and qRT-PCR was run in quadruplicate using TaqMan assays on a QuantStudio 12K Flex Real-Time PCR System [4]. Genes of interest included markers of inflammatory (TNF-α, IL-1b, IL- 6, and IL-10, Prostaglandin E2, CD68, CD163, and CD45), tendon repair (TGF-β1, TGF-β3, and VEGFb) and tendon remodeling (COL I, III, and IV, MMPs -2,-3,-8 and -10, tenascin, tenomodulin, and aggrecan). Expression was normalized to the internal control (GAPDH) and fold change was calculated by normalizing treatment groups to the untreated control, No_BiLDS. ELISA for TNF-α and IL-6 was performed on protein isolates from the excised tendons and for IBP in serum samples collected at 4 and 8 weeks (n=6/group/timepoint). *Tensile Mechanical Testing*: The cross-sectional area of the left intact supraspinatus tendons from animals sacrificed at 4 and 8 weeks (n=12/group/timepoint) was measured using a custom laser device. Ex vivo tensile testing was performed as follows: preload, preconditioning, stress relaxation, and ramp to failure. Modulus, stiffness, maximum load, and maximum stress were computed. *Statistics:* Two-way ANOVA and normality tests were performed on all datasets. To compare between groups at each timepoint, one-way ANOVA or Kruskall-Wallis tests were performed, depending on normality. To compare over time within each treatment group, Welch's t-tests or Mann-Whitney U tests were performed. Significance was set at $p<0.05$ (*); ** denotes $p<0.01$ and ***denotes $p<0.001$.

RESULTS: There were no statistically significant differences in cell shape, cellularity, expression of tendon healing genes or IL-6 cytokine expression between the treatment groups at each timepoint (data not shown). IBP was undetectable in the serum of all animals at 4 and 8 weeks (data not shown). Tendons treated with BiLDS_IBP expressed significantly less TNF-α compared to untreated tendons, No_BiLDS, at 8 weeks and both BiLDS groups decreased in TNF- α at the protein level over time (Fig. 1A). Stiffness, modulus, maximum stress, and maximum load of the untreated tendons (No_BiLDS) were significantly greater than in either of the treated groups, BiLDS and BiLDS_IBP, at 4 weeks (Fig. 1B-D). Stiffness, maximum stress, and maximum load increased for all groups over time (Fig. 1B & 2D). Modulus and maximum stress of the treated tendons in the BiLDS group were lower in comparison to the No_BiLDS group at 8 weeks, but there were no differences in these parameters between the No_BiLDS and BiLDS_IBP groups at 8 weeks (Fig. 1C & 1D). There were no significant differences in stiffness (Fig. 1B) and maximum load at 8 weeks or in tendon cross-sectional area at either 4 or 8 weeks (data not shown).

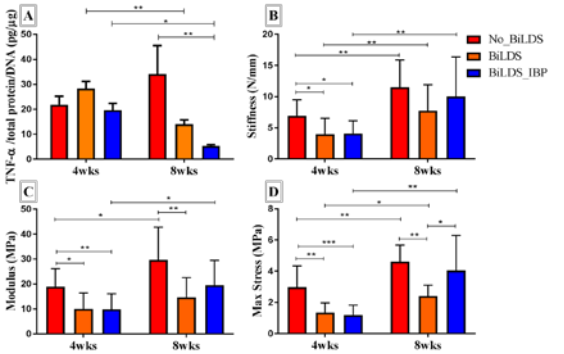

Figure 1. (A) Treated tendons, BiLDS and BiLDS_IBP, significantly decreased in cytokine expression of TNF-α over time and IBP-treated tendons expressed significantly less TNF-α than the untreated tendons, No_BiLDS, at 8 weeks. The untreated tendons, No_BiLDS, exhibited significantly greater (B) stiffness, (C) modulus, and (D) maximum stress at 4 weeks in comparison to the treated tendons, BiLDS and BiLDS_IBP. Data presented as mean ± SD. (*p<0.05, **p<0.01, ***p<0.001)

DISCUSSION: Although the use of BiLDS and BiLDS_IBP was not therapeutically beneficial for rat rotator cuff healing in terms of mechanics, the release of IBP from BiLDS significantly decreased pro-inflammatory signaling in the late healing phase. There were no substantial changes in gene expression 1 week post-repair with either treatment (BiLDS or BiLDS_IBP) compared to standard surgical repair (No_BiLDS). Therefore, we are unable to conclude the biological effect of the BiLDS with and without IBP on tendon repair at this time. Further investigation is ongoing to evaluate additional tendon healing markers at the protein level up to 8 weeks post-repair. Mechanical testing results indicated both BiLDS and BiLDS_IBP were detrimental to tendon mechanics compared to surgical repair alone, especially at early timepoints. Previous work revealed no significant differences in structural properties after surgical repair with and without the implantation of a single layered PCL scaffold in a rat rotator cuff injury and repair model [5]. Therefore, the decreased mechanics seen with the use of BiLDS in this study may be due to the increased size of the BiLDS compared to a single-layer PCL scaffold. Implanting a substantially thicker scaffold into the tight subacromial space in the rat shoulder may have caused supraspinatus impingement and negatively affected early tendon healing. Despite this, the BiLDS and BiLDS_IBP constructs remained intact, led to decreased pro-inflammatory expression over time, and recovered the tendon structural properties by 8 weeks. Future studies are required to elucidate the effect of the BiLDS and BiLDS_IBP on tendon mechanics at later timepoints and in larger defects in which supplementation with a scaffold may be necessary to stabilize repair.

SIGNIFICANCE: This study investigates a biocompatible nanofibrous bilayer delivery system (BiLDS) for localized delivery of ibuprofen to mitigate inflammation in a rat rotator cuff repair model. Further evaluation is necessary to elucidate the beneficial effects of the system in a larger animal model.

REFERENCES: [1] Taylor et al., ORS 2018 (Poster No. 0356), [2] Kim et al., ORS 2018 (Poster No. 0781), [3] Huegel et al., J Orthop Res., 35:1250-1257, 2017, [4] Reno et al., Biotechniques, 22:1082-1086, 1997, [5] Beason et al., JSES, 21:245-250, 2012.

ACKNOWLEDGEMENTS: This project was funded by a VA Merit Grant (O0979-R), the Penn Center for Musculoskeletal Disorders (NIH/NIAMS P30 AR069619), and a Vice Provost for Research fellowship to B. Taylor. We thank Adnan Cheema, Corinne Riggin, and Hetty Rodriquez for their assistance.

Scleraxis Targeted Deletion of Collagen XI Affects Mouse Tendon Mechanical Properties

Yaping Ye[1], Snehal S. Shetye[1], Ryan Leiphart[1], David E. Birk[2], Louis J. Soslowsky[1]
[1]Mckay Orthopaedic Research Laboratory, University of Pennsylvania, Philadelphia, PA
[2]Department of Molecular Pharmacology & Physiology, University of South Florida, Tampa, FL

Disclosures: Y Ye (N), SS Shetye (N), R Leiphart (N), DE Birk (N), LJ Soslowsky (N)

INTRODUCTION: Type II Stickler syndrome is associated with abnormal mutations in the COL11A1 gene and in patients, manifests with a distinctive facial appearance, eye abnormalities, hearing impairment, and joint disorders [1]. In addition, polymorphisms of the collagen XI gene have been recently linked to tendinopathy [2]. Despite being a quantitatively minor component in tendons, the fibril-forming collagen XI plays an essential regulatory role in initial fibril assembly, fiber organization and establishment of tendon structure and function [3]. However, the role of collagen XI in regulating tendon-specific mechanical response has not yet been elucidated. Therefore, the objective of this study was to determine the contribution of collagen XI to the establishment of mechanical properties in mouse Achilles (ACH) and flexor digitorum longus (FDL) tendons. We hypothesized that the absence of collagen XI would result in a diminished structural and material mechanical response of the ACH and FDL tendons.

METHODS: Male *Col11a1*$^{+/+}$ control (WT, n=12) and conditional *Scx*- specific *Col11a1*$^{\Delta Ten/\Delta Ten}$ mice (*Col11a1*$^{\Delta Ten/\Delta Ten}$, n=15) were utilized (IACUC approved). Following euthanasia at 60 days postnatal, the FDL and ACH were dissected and prepared for mechanical testing as described [4]. Briefly, 10mm FDL tendon sections were carefully removed from the ventral aspect of the mouse foot and cleaned free of soft tissue. Verhoeff's stain lines were placed 2.5mm apart within the mid-substance to track strain optically with a final free tendon length of 5mm. ACH tendons were dissected under a dissection scope and cleaned of excess tissue leaving only the calcaneus and tendon. Verhoeff's stain lines were placed 2mm apart within the mid-substance to track strain optically. Cross-sectional area was measured using a custom laser device. Samples were placed in a phosphate buffered saline bath and loaded in a materials testing system. Stiffness was calculated as the slope of the linear region of the load-displacement curve during a ramp to failure at 0.3%/s. Modulus was calculated as the slope of the linear region of the stress-strain curve. Stress relaxation (%) was calculated from a 600s stress relaxation test at 5% strain for FDL and 6% strain for ACH. After satisfying normality and equality of variance conditions, two-tailed Student's t-tests were performed with significance set at $p<0.05$.

RESULTS: Cross-sectional area was significantly reduced in both *Col11a1*$^{\Delta Ten/\Delta Ten}$ ACH and FDL tendons (Fig. 1A). However, percent stress relaxation was not affected by the absence of collagen XI in the ACH and FDL (Fig. 1B). Both maximum load and stiffness were reduced in the Col11a1$^{\Delta Ten/\Delta Ten}$ ACH and FDL (Fig. 1C-D). Maximum stress was significantly reduced in the *Col11a1*$^{\Delta Ten/\Delta Ten}$ group for ACH and FDL (Fig. 2A). The modulus was reduced in the *Col11a1*$^{\Delta Ten/\Delta Ten}$ group for FDL but not for the ACH.

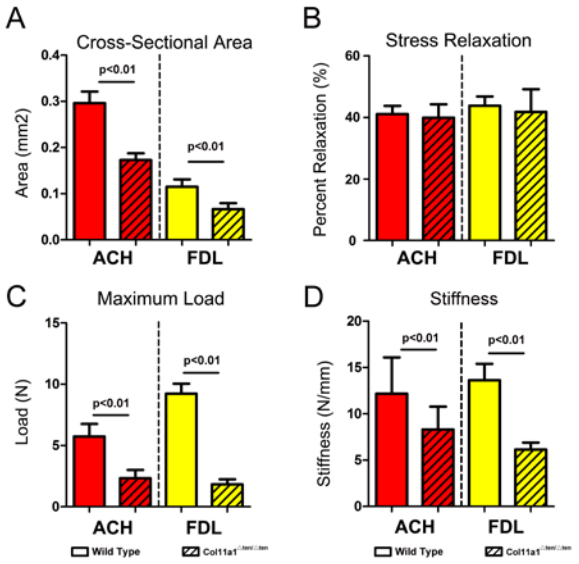

Figure 1: (A) Cross-sectional area was decreased in the *Col11a1*$^{\Delta Ten/\Delta Ten}$ group compared to the wild type group in ACH and FDL. (B) Percent relaxation was not altered with collagen XI removal in ACH and FDL. (C) Maximum load was decreased in the *Col11a1*$^{\Delta Ten/\Delta Ten}$ group compared to the wild type group in ACH and FDL. (D) Modulus was decreased in the *Col11a1*$^{\Delta Ten/\Delta Ten}$ group compared to the wild type group in ACH and FDL. Data presented as mean ± standard deviation.

DISCUSSION: This study investigated how collagen XI deficiency affects the mechanical response of the Achilles and flexor digitorum longus tendons. Overall, *Col11a1*$^{\Delta Ten/\Delta Ten}$ ACH and FDL tendons were structurally and materially inferior to their wild type counterparts. Collagen XI deficient tendons were smaller and thus had lower tendon stiffness and load to failure values. In addition to weaker structural properties, collagen XI deficiency also altered tendon material quality, with lower maximum stress values in both ACH and FDL tendons. Interestingly, a less severe phenotype was observed in the Achilles tendon with no difference observed in modulus. Similar tendon-specific phenotypic manifestations have been previously observed with collagen V, another fibril-forming collagen [4]. These results support the clinically observed phenotype in Stickler syndrome patients, and also suggest a possible role of collagen XI in tendinopathy. This study is not without limitations. This study only investigated the ACH and FDL tendons, but did not measure other tissues such as joint capsule or cartilage. This study only measured the response of tendons to load at the macroscale level, but there could also be changes in the response to load at the fiber or fibril level. Despite these limitations, this study provides surprising evidence that Collagen XI plays a significant role in the mechanical properties of ACH and FDL.

SIGNIFICANCE/CLINICAL RELEVANCE: This study demonstrates that collagen XI plays an important role in the mechanical properties of mouse ACH and FDL tendon. Collagen XI could be considered as a potential therapeutic target for improving the mechanical integrity of tendons.

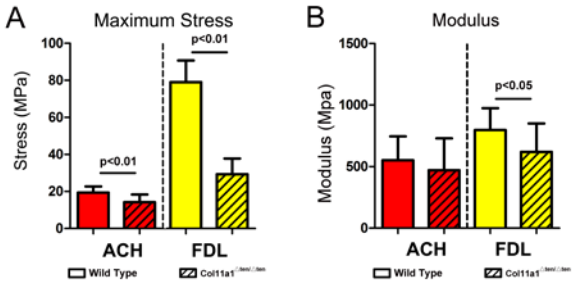

Figure 2: (A) Maximum stress was decreased in the *Col11a1*$^{\Delta Ten/\Delta Ten}$ group compared to the wild type group in ACH and FDL. (B) Modulus was decreased in the *Col11a1*$^{\Delta Ten/\Delta Ten}$ group compared to the wild type group only for the FDL. Data presented as mean ± standard deviation.

REFERENCES: [1] Cattalini M et al., Pediatr Rheumatol Online J, 2015. [2] Hay M et al., Br J Sports Med, 2013. [3] Mienaltowski MJ et al., Adv Exp Med Biol, 2014. [4] Connizzo BK et al., J Orthop Res, 2015.

ACKNOWLEDGEMENTS: This study was supported by the Penn Center for Musculoskeletal Disorders (NIH/NIAMS P30 AR069619).